Meteor-Berichte

Yucatan Throughflow

Cruise No. M94

March 12 – March 26, 2013
Balboa (Panama) – Kingston (Jamaica)

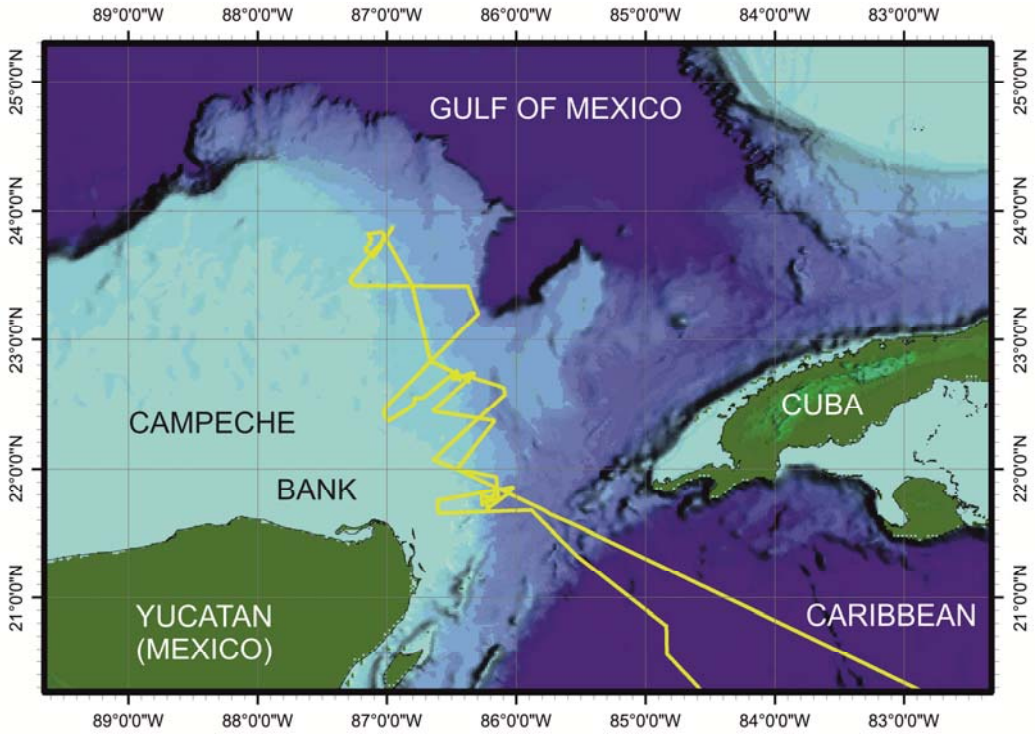

C. Hübscher, D. Nürnberg,
M. Al Hseinat, M. Alvarez García, Z. Erdem, N. Gehre, A. Jentzen, C. Kalvelage, C. Karas, B. Kimmel, T. Mildner, A. O. Ortiz, A. O. Parker, A. Petersen, A. Raeke, S. Reiche, M. Schmidt, B. Weiß, D. Wolf

Editorial Assistance:

DFG-Senatskommission für Ozeanographie
MARUM - Zentrum für Marine Umweltwissenschaften der Universität Bremen

2014

The METEOR-Berichte are published at irregular intervals. They are working papers for people who are occupied with the respective expedition and are intended as reports for the funding institutions. The opinions expressed in the METEOR-Berichte are only those of the authors.

The METEOR expeditions are funded by the *Deutsche Forschungsgemeinschaft (DFG)* and the *Bundesministerium für Bildung und Forschung (BMBF)*.

Editor:
DFG-Senatskommission für Ozeanographie
c/o MARUM – Zentrum für Marine Umweltwissenschaften
Universität Bremen
Leobener Strasse
28359 Bremen

Author:
Prof. Dr. Christian Hübscher
Universität Hamburg
Institut für Geophysik
Bundesstrasse 55
20146 Hamburg

Telefon:040-428385184
Telefax:040-428385441
e-mail:christian.huebscher@zmaw.de

Citation: C. Hübscher, D. Nürnberg, M. Al Hseinat, M. Alvarez García, Z. Erdem, N. Gehre, A. Jentzen, C. Kalvelage, C. Karas, B. Kimmel, T. Mildner, A. O. Ortiz, A. O. Parker, A. Petersen, A. Raeke, S. Reiche, M. Schmidt, B. Weiß, D. Wolf (2014) Yucatan Throughflow - Cruise No. M94 – March 12 – March 26, 2013 – Balboa (Panama) – Kingston (Jamaica). METEOR-Berichte, M94, 32 pp., DFG-Senatskommission für Ozeanographie, DOI:10.2312/cr_m94

ISSN 2195-8475

Table of Contents

1 Summary

The Loop Current and its associated eddy-shedding in the Gulf of Mexico are mediating the oceanic heat and salt flux from the Caribbean into the Atlantic Ocean via Yucatan Strait. Changes in Yucatan Strait surface and intermediate through flow over geological timescales in relation to sea level, through flow velocity, and atmospheric circulation are not well constrained to date. The main objective of the geological sediment sampling program was to establish spatially and temporally high-resolving reconstructions of the Late Pleistocene surface, subsurface and intermediate water variability, in relation to the Loop Current variations and related eddy shedding, Antarctic Intermediate Water migrations, and changes in the Atlantic Meridional Overturning Circulation. The multi-channel seismic program was designed to establish a sequence stratigraphic framework for current controlled sediment formations which reflect the onset and intensification of the Gulfstream as well as Mid-Pleistocene climate transition. We focused on the main inflow area of Caribbean waters into the Gulf of Mexico, namely Yucatan Strait, and adjacent areas influenced by the Loop Current, i.e., the northeastern slope of Campeche Bank.

Zusammenfassung

Das Loop-Stromsystem mit seinen großflächigen, sich im Golf von Mexiko abtrennenden Wirbeln regelt den ozeanischen Wärme- und Salztransfer aus der Karibik über die Yucatan Straße in den Atlantischen Ozean. Die Veränderlichkeit des oberflächlichen, oberflächennahen und intermediären Durchstroms im Bereich der Yucatan Straße ist auf geologischen Zeitskalen wenig bekannt. Das geologische Arbeitsprogramm hatte zum Ziel, die Dynamik des Yucatan Durchstromes mit hoher zeitlicher Auflösung für das Pleistozän zu rekonstruieren und in Beziehung zur Veränderlichkeit des Loop-Stromsystems und dessen Wirbelentstehung, zur Ausdehnung des Antarktischen Zwischenwassers (AAIW) und zu Veränderungen in der thermohaline Zirkulation im Atlantik – dem Golfstrom - zu setzen. Das mehrkanal-seismische Programm diente der Erarbeitung eines sequenzstratigraphischen Rahmenwerks für strömungskontrollierte Ablagerungen, welche das Einsetzen und die Verstärkung des Golfsstromes sowie die Mittel-Pleistozäne Klimavariation widerspiegeln. Räumlich fokussierten wir uns auf das Einstromgebiet karibischer Wassermassen in den Golf von Mexiko in der Yucatan-Straße und denjenigen benachbarten Gebieten, die unter dem Einfluss des Loop Currents stehen, als den Nordosthang der Campeche Bank.

2 Participants

Name, academic title	Discipline	Institution
Hübscher, Christian, Prof. Dr.	Geophysics, Chief Scientist	IfG
Nürnberg, Dirk, Prof. Dr.	Geology, Senior Scientist	GEOMAR
Al Hseinat, Mu'ayyad	Geophysics	IfG
Kalvelage, Claudia	Geophysics	IfG
Kimmel, Bastian	Geophysics	IfG
Reiche, Sönke	Geophysics	IfG
Weiß, Benedikt	Geophysics	IfG
Wolf, Daniela	Geophysics	IfG
Erdem, Zeynep	Geology	GEOMAR
Gehre, Nadine	Geology	GEOMAR
Jentzen, Anna	Geology	GEOMAR
Karas, Cyrus, Dr.	Geology	IfGF
Petersen, Asmus	Geology	GEOMAR
Mildner, Tanja	Geology	IfM
Ortiz, Aramis Olivos, Dr.	Geology, Observer	CEUNIVO
Álvarez García, Maria, Dr.	Geology, Observer	CEUNIVO
Schmidt, Matthew, Prof. Dr.	Guest Scientist	AMU
Parker, Andrew O.	Guest Scientist	AMU
Andreas Raeke	Meteorology	DWD

AMU
Texas A&M University
Department of Oceanography
MS 3146, Texas A&M University
College Station
Texas 77843-3146, USA

CEUNIVO
Centro Universitario de Investigaciones Oceanológicas
Universidad de Colima
Colonia El Naranjo. C.P. 28860
Manzanillo, Colima, México

DWD
Deutscher Wetterdienst
Seeschifffahrtsberatung
Bernhard-Nocht-Straße 76
20359 Hamburg / Germany

GEOMAR
Helmholtz-Zentrum für Ozeanforschung Kiel
Düsternbrooker Weg 20
24105 Kiel / Germany

IFG
Institut für Geophysik
Universität Hamburg
Bundesstraße 55
20146 Hamburg / Germany

IfGF
Institut für Geowissenschaften
Johann Wolfgang Goethe-Universität
Altenhöferallee 1
60438 Frankfurt am Main / Germany

IfM
Institut für Meereskunde
Universität Hamburg
Bundesstrasse 55
20146 Hamburg / Germany

3 Research Program

3.1 Paleoceanographic Objectives

The overarching goal of the proposed RV METEOR campaign was to unravel the Loop Current dynamics, related eddy shedding and countercurrents, and AAIW variability during the course of glacials, deglaciations, and interglacials in the Yucatan Strait area. In particular, we attempted to constrain the relation of Yucatan Strait Throughflow dynamics to sea level fluctuations, the variability of the Atlantic Meridional Overturning Circulation (AMOC), and migrations of the Inner Tropical Convergence Zone (ITCZ). During M94, we focused on the main inflow area of Caribbean waters into the Gulf of Mexico, namely Yucatan Strait, and adjacent areas influenced by the Loop Current, e.g. the northeastern slope of Campeche Bank. We used RV METEOR in order

- to recover long and high-quality sediment cores from mounded elongated sediment drift complexes in the proposed areas in order to establish spatially and temporally high-resolving reconstructions of surface to intermediate water variability. The core sites were selected from hydroacoustic profiles (PARASOUND) mapped during RV METEOR cruise M78/1 in 2009 (Schönfeld et al., 2009) and by intense high-quality hydroacoustic and multi-channel seismic surveying during RV METEOR cruise M94. By applying state-of-the-art geochemical, sedimentological, and micropaleontological proxies, we will be able to further elucidate the Yucatan Strait Throughflow dynamics at different water depths and improve existing paleoreconstructions of surface to intermediate water variability during glacial, deglacial and interglacial periods of the late Pleistocene.
- to collect high-resolution reflection seismic, PARASOUND and multi-beam data to unravel the impact of the Loop Current, Eddy shedding and counter currents on middle and lower slope drift deposits. We hypothesize that these contourites reflect the late Miocene/early Pliocene onset and the intensification of the Gulfstream as well as the Mid-Pleistocene Transition. These data will further increase our knowledge about scalloped carbonate bank margins, related mass failures and fluid-carbonate interactions.
- to investigate the habitat of recent living planktonic foraminifera and to analyze stable isotopes and trace metals of the tests in relation to the ambient seawater conditions in the Yucatan Strait. Therefore, living planktonic foraminifera were collected with an Apstein net from different water depths. Near surface plankton samples and water samples were taken by using the ship´s pump and hydrographic measurements were recorded with the shipboard thermosalinograph during the cruise M94.

Based on the geological and geophysical data collected during the cruise we will address the following major issues:

- Impact of the Loop Current extent and eddy shedding on the Yucatan Strait Throughflow; surface, subsurface and intermediate water hydrography and its change through time.
  We intend to reconstruct and to understand the formation of the Loop Current and its eddy shedding in the Gulf of Mexico, the time history of hydrographic changes in the Yucatan Strait Throughflow and the Gulf of Mexico, and its relation to the AMOC.
- Role of Antarctic Intermediate Water in the Yucatan Strait Throughflow area
  We will track the northward migration of AAIW during the late Pleistocene. We will investigate whether there was an increasing advection during deglacial cool periods when the AMOC was weak. We will disentangle interactions between AAIW from the south, and both deep-reaching Loop Current eddies and related countercurrents from N-Atlantic intermediate waters.
- Sediment drift evolution in Yucatan Strait and on Campeche Bank
  We will study in greater detail the evolution of contourite and sediment drifts and their time of formation. Emphasis will be given to relationships with bottom current dynamics, and

paleoceanographic and paleoclimatic events like the onset of the Gulfstream, its intensification and the Mid-Pleistocene Transition.

- Formation of erosional unconformities at the northeastern Campeche Bank
  The presence of prominent erosional unconformities at Campeche Bank implies a dramatic change of the Loop Current in the eastern Gulf of Mexico and in the Yucatan Strait Throughflow pattern. We will attempt to sample and date the unconformity and test the hypothesis, whether its formation is related to the "Mid-Pleistocene Revolution". This profound change in the climate system at ~0.9 Ma describes the transition of earth´s climate from a more linear to a strongly non-linear climate system with an abrupt increase of the 100-kyr-cycle amplitude, which possibly led to the first glacial decrease in NADW production. The sea level drop of ~30 m at that time would have narrowed and accelerated the Yucatan Strait Throughflow. From interpretation of multi-channel profiles with a much higher depth penetration than PARASOUND we will find out whether the erosional unconformity and, consequently, the dramatic change of the Loop Current system was a single or multiple event.
- Teleconnection between Pleistocene to Holocene oceanographic changes in Yucatan Strait and the Central American climate
  The past variability in ocean properties will be compared to regional and global climate changes with reference to migrations of the ITCZ. In particular, we will document correlations and synchronies of local events in the Yucatan Strait area with existing continental climate records from Yucatan Peninsula (e.g., Lake Petén Itzá records, ~17°N ~90°W) and Mexican highlands (e.g. dendrochronological records).
- Impact of ITCZ migrations on precipitations patterns and continental erosion rates
  We will document the past variability of the continental areas submitted to erosion, in particular during past warm climate periods. These analyses will help to constrain the extreme fluctuations in the rainfall patterns and the variability of past terrigenous supply through fluvial systems in response to ITCZ migrations. Our results will improve the knowledge on the past variability of the continental hydrological regime and will permit to propose synoptic scenarios of the associated moisture transfer and the atmospheric configuration.
- Impact of deglacial "superflooding"
  We will address the issue of deglacial Mississippi megadischarge events influencing the Gulf of Mexico surface salinity. The impact of such events was evidenced in the western Gulf of Mexico and south of the Mississippi Delta (Orca Basin). It is unknown, however, how far such superflooding-related salinity anomalies propagated southward and eastward. We will address, how the little - if any - imprint of the superflooding on the AMOC can be explained. Does freshwater discharge fade out into the deep ocean?

3.2 Modern Hydrographic Setting in the Study Area

The Western Hemisphere Warm Pool (WHWP), which is characterized by extremely high mean annual sea surface temperatures and related feedback mechanisms (i.e. atmospheric circulation, cloud formation, greenhouse warming, SST-dependant and CO_2-uptake), not only supplies tropical heat and moisture to the atmosphere, but is regarded as the main heat and salt reservoir to be transferred to the North Atlantic *via* the Loop Current / Gulf Stream system (Fig. 3.2.1).

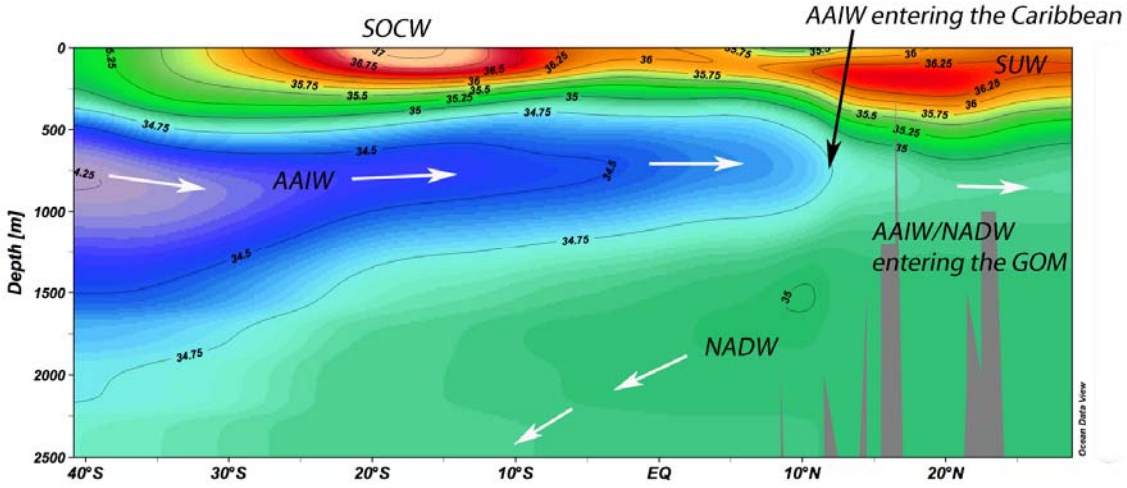

Fig. 3.2.1. S-N-trending salinity-profile from ~40°S to ~28°N showing AAIW entering the Gulf of Mexico via Yucatan Strait, Subtropical Underwater (SUW), and North Atlantic Deep Water (NADW). Image produced with Ocean Data View.

This northward flowing Western Boundary Current is a key component in thermohaline circulation. Of prime interest to both the paleoceanographic community and to climate projections is to understand how WHWP dynamics and changes in the thermohaline circulation including re-organizations in surface currents (e.g., Loop Current), deep water masses (e.g., North Atlantic Deep Water, NADW) and intermediate water masses (e.g., Subtropical Underwater, SUW; AAIW) operate and interact on short time scales (Figure 3.2.2). Thereby, the position and the seasonal variation of the ITCZ influences both hydrology and climate in the Caribbean area as ITCZ migrations are causing changes in the tropical wind field and the strength of the AMOC.

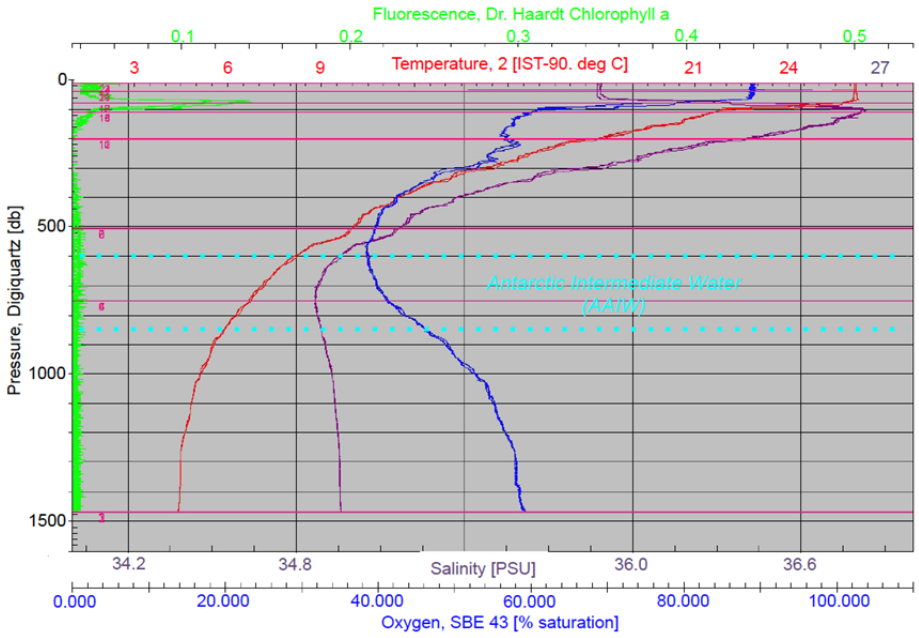

Fig. 3.2.2 CTD-profile M78-166-1 from Yucatan Strait (28.02. 2009, 11:20; Lat. 21° 40.79' N; Long. 86° 9.92' W; water depth: 1541m). Hatched lines indicate Antarctic Intermediate Water, characterized by a subtle salinity decrease. Data published in Schönfeld et al. (2012).

Surface currents

Caribbean surface waters pass the Yucatan channel and flow into the Gulf of Mexico *via* the Loop Current (Pickard and Emery, 1982) (Figure 3.2.1), which is clearly expressed in sea-surface height (e.g., Sturges and Evans, 1983). Although causation is not well understood, coherencies between Loop Current retraction and extension, seasonal migrations of the ITCZ, the related wind system and changes in the thermohaline circulation are corroborated by model simulations (e.g., Johns et al., 2002), which denote both, a purely wind-driven Caribbean inflow through the Caribbean Passages and an overturning-related inflow.

A characteristic feature of the Loop Current is the shedding of anticyclonic eddies. The eddy formation is critical for both, regional climate in the Gulf of Mexico and large-scale transports towards high northern latitudes with far-reaching consequences for the climate in western and central Europe. The eddies are generated aperiodically every 3 to 21 months, with an average shedding time of 9.5 months (Zavala-Hidalgo et al., 2006). They may reach down to ~1200 m, thereby influencing deep water inflow into the Gulf of Mexico as well as compensating southward-directed deep flows (Bunge et al., 2002). Eddy shedding is a strongly non-linear process and its dynamics are not well understood. Its forcing appears to be related to a suite of oceanographic forcing fields such as the Yucatan Channel throughflow (Ezer et al., 2003; Oey, 2004; Oey et al., 2003), the Florida Current and North Brazil Current variability, as well as synoptic Metereological forcing variability (Romanou et al., 2004). The detachment of an eddy from the Yucatan Strait throughflow may take weeks and often a developing eddy reattaches to the Loop Current.

Intermediate and deep water masses

The Caribbean deep and intermediate water masses form from the inflow of Atlantic water masses, which enter the Caribbean *via* deep-water passages (Anegada Passage, Windward Passage, Antilles passages). North Atlantic Intermediate Water (NAIW), Upper North Atlantic Deep Water (UNADW), Mediterranean Outflow Water (MOW) and Antarctic Intermediate Water (AAIW) serve as main sources for the Caribbean Intermediate Water. In the southern Caribbean Basin, AAIW may contribute up to 30% (Haddad and Droxler, 1996). From model calculations, Worthington (1971) postulated an AAIW inflow of 10 Sv into the Caribbean.

Low saline (<34 psu) and nutrient-enriched AAIW form at ~50°S in the S-Atlantic and SE-Pacific and then flows northward. It is identified in the Gulf of Mexico at depths of 500-1000 m, underlain by North Atlantic Deep Water (NADW, ~35 psu). It largely contributes to the eddy shedding Loop Current. AAIW is overlain by higher saline (~37 psu) Subtropical Underwater (SUW). The uppermost ~200 m are characterized by mixed Surface Water (SW).

In the Yucatan Straits and the southern Gulf of Mexico, the hydrography at intermediate water depths is governed by deep Loop Current eddies, northbound intrusions of Antarctic Intermediate Water (AAIW), and southbound counter-currents related to the Loop Current. Interactions between these current regimes affected both erosional features at intermediate depths and elongated sediment drift mound complexes on the sea floor. These sedimentary structures have been previously identified in the Yucatan Straits, on the northern slope of Campeche Bank, and on the W-Florida continental slope based on hydroacoustic data (Hübscher et al., 2010). The presence of these structures may indicate a deep, high energy environment of basinwide significance (Hübscher et al., 2010). However, the age of regional unconformities and sedimentary drifts is unknown, and the appropriate sediment cores that would help determine the history of intermediate water circulation dynamics do not exist.

3.3 Late Pleistocene to Holocene Paleoceanography

Changes in Yucatan Strait Throughflow over geological timescales are not well constrained to date. Geological records from the northeastern Gulf of Mexico revealed that the Loop Current

was subject to profound changes on glacial/interglacial timescales (Nürnberg et al., 2008). Deglacial changes in Gulf of Mexico sea surface temperature and salinity appear to be coeval with, but significantly larger than those in the central Caribbean (Schmidt et al., 2006). Data from paleoarchives and model results suggest that the continuous and stronger surface warming in the Gulf during the glacial terminations was linked to the onset and increase of eddy-shedding by the Loop Current related to deglacial sea level rise, Yucatan Strait throughflow velocity, and changes in the atmospheric circulation (see Chapter 3.2). Surface freshening occurs during glacial periods and deglacial cool events and was most likely related to enhanced and eastward directed Mississippi river discharge.

According to Blunier et al. (1998) and Rühlemann et al. (1999), the Atlantic heat transport into high northern latitudes was closely coupled to northern NADW formation (Keigwin et al., 1991; Driscoll and Haug, 1998). During times of enhanced melt water supply into the North Atlantic (e.g., Younger Dryas and Heinrich 1 event), NADW formation decreased, thermohaline circulation slowed down or even collapsed (evidenced by the McManus et al., (2004) $^{231}Pa/^{230}Th$-record from Bermuda Rise), and the transequatorial transfer of warm subtropical waters into the North Atlantic diminished, causing considerable cooling in the North Atlantic (e.g., Ganopolski et al., 1998; Bard et al., 2000). The tropical/subtropical Atlantic, instead, warmed up as shown by Tobago Basin alkenon temperatures (Rühlemann et al., 1999).

During the prominent deglacial climatic reversals, Rühlemann et al. (2004) infer a warming of intermediate waters in Tobago Basin and along the Brazilian margin, caused by a reduced ventilation of cold intermediate and deep waters in conjunction with downward mixing of heat from the thermocline. How this relates to changes in the spread of AAIW is a matter of debate. Mid-depth $\delta^{13}C$ and Cd/Ca records from the Atlantic suggest the presence of nutrient-rich southern source waters at intermediate water depths during the Heinrich 1 and Younger Dryas cold events. Pahnke et al. (2008) postulated a northward migration of AAIW during the deglacial cold phases Heinrich 1 and the YD, at times when the southward spreading of NADW ceased. Following these cool events, the AMOC rapidly resumed, concurrent with the deglacial warming events. Overall, it is not sufficiently known, how far less saline and nutrient-rich AAIW invaded into the Caribbean and further into the Gulf of Mexico, mainly due to the lack of mid-depth sediment records from these areas.

3.4 Paleoceanographic and Paleoclimate Relevance of Gulfstream Onset and Intensification

The closure of the Central American Seaway through the Panamanian Isthmus in the early Pliocene led to the onset and intensification of the Gulf Stream. The intensification of Northern Hemisphere glaciation (NHG) since 3 Ma, playing a major role in the modification of Pliocene climate and oceanography (for an overview see, e.g., Steph et al. 2006 and references therein), was one of the consequences.

Fig. 3.4.1 The closure of the Panamanian Isthmus triggered the onset and intensification of the Gulf Stream (from Haug et al., 2004).

Closure-induced changes in global thermohaline circulation have been considered to be the cause either for the onset (Berggren and Hollister, 1974), for the delay (Berger and Wefer, 1996), or for setting the preconditions for NHG (Haug and Tiedemann, 1998; Driscoll and Haug, 1998). While the link between closure and climate is still a matter of debate, paleoceanographic studies suggest a close link between the formation of the isthmus and major oceanographic changes during the early Pliocene (4.7–4.2 Ma), when the shoaling of the Panamanian sill reached a critical threshold for upper ocean water mass exchange (Haug et al., 2001). Restricted exchange of surface water led to the establishment of the modern Atlantic/Pacific salinity contrast that may be linked to atmospheric net freshwater transport from the tropical Atlantic and Caribbe- an into the equatorial east Pacific (e.g., Broecker and Denton, 1989; Jousaumme et al., 1986). In addition, results from General Circulation Models and paleoceanographic studies suggest a reorganization of equatorial Pacific surface circulation, and an increased volume transport of heat and salt into the North Atlantic via an intensified Gulf Stream, favoring North Atlantic Deep Water (NADW) formation and Atlantic carbonate preservation (e.g., Haug and Tiedemann, 1998; Haug et al., 2001; Prange and Schulz, 2004).

4 Narrative of the Cruise

The unloading of M93 equipment as well as the loading of the M94 gear was initially scheduled for 10th of March. However, there was no berth available and METEOR was on anchor off Panama City until noon of March 11th. The scientific party boarded the vessel on the 12th where they were welcomed by captain and crew. The entire port operations were done the next day until 6 p.m. Four containers were unstuffed on the pier and alongside the vessel by the help of stevedores, crew and scientists. Since the Panama Channel passage had to be postponed by one day we left berth and anchored off the first channel lock. While still on anchor, the 13th of March was used to install the equipment in the labs. Around 8 pm the pilot came on board and METEOR approached the Locks of Miraflores. The channel was passed during the night and we all watched the show.

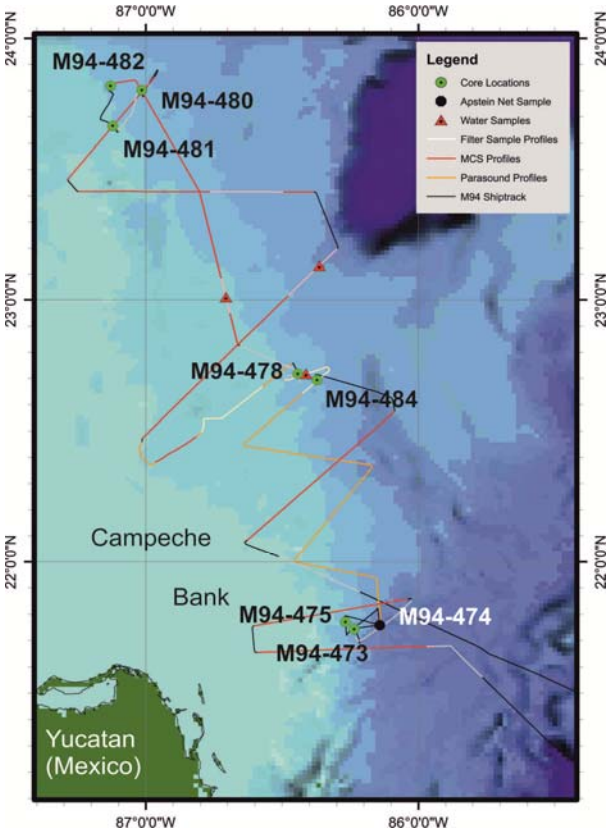

Fig. 4.1 M94 station chart showing sediment coring (black numbers) and plankton net locations (white number). Seismic profiles see Fig. 5.3.2.1.

After entering the Caribbean Sea next morning the vessel became a bit shaky and a few of the scientific party needed some time to get used to it. Owing to the warm water the cooling system of the ship's engine was clogged by biomass so we had to reduce speed for a couple of hours. The digital streamer was deployed for two hours in order to install the analogue-digital converters. On March 15th and 16th we proceeded with our lab installations while steaming northwards on our transit across the Caribbean Sea.

We reached our first working area on Sunday March 17th in the Yucatan Strait between Yucatan Peninsula and Cuba where we started with two geophysical profiles using multi-channel seismics, the parametric subbottom profiler PARASOUND and the EM122 multi-beam system in order to investigate depositional processes on the eastern slope of the Campeche Bank between Yucatan and Cuba. Afterwards and on Monday (March 18) we took two piston cores in order to study sediment deposits controlled by the northward flowing Antarctic Intermediate Water and by the southward flowing counter currents. In between, the plankton net had been utilized. Late evening, the sound velocity probe helped to get a detailed sound velocity depth profile needed for the multi-beam system. During the following night the upper and middle slope of the eastern Campeche Bank was surveyed with the hydroacoustic systems in order to understand the impact of the northward flowing Loop Currents on Late-Pleistocene to Holocene sediments as a function of the distance to the Yucatan Strait. One piston core station had been selected for the 19th based on the previous hydroacoustic surveys on the southern Campeche slope. Late afternoon same day the multichannel equipment was deployed and three seismic profiles zigzagging across the Campeche slope were completed until 21st early morning. Three piston cores were taken in order to get both a high-resolution record of late-Pleistocene strata and to age constrain an unconformity which is considered to represent a marker for a significant change in the Loop Current characteristics and – consequently – for a climatic change at least in the Central American realm. In the night to the 22nd a contour parallel seismic profile crossing three previous profiles was measured in order to link the seismo-stratigraphic sequences identified before. The piston corer was applied a last time during this day and the night to the 23rd was used for a final seismic profile crossing a canyon on the lower Campeche slope and continuing upslope in order to close a gap in the already accomplished profile grid. All scientific measurements stopped on the 23rd at 7:00 am local time when we started our southbound transit to Kingston / Jamaica.

The transit lasted until the 26th in the morning when the ship stopped south-west of Kingston for a person overboard manoeuvre. The pilot entered the vessel at 13:00 and early afternoon the ship berthed at Kingston harbour. During a reception aboard METEOR we have been honoured by visits of the German ambassador Mr. Beck and, a.o., representatives of the International Seabed Authority ISA and Kingston Port authorities.

5 Preliminary Results

5.1 Hydroacoustics

The hydroacoustic instruments comprised a parametric sediment sub-bottom profiler and two swath sounders. Except for the OBS-deployment/recovery periods the PARASOUND system was continuously operated in all working areas. The swath sounders were used according to predominant water depths.

The hull mounted PARASOUND system sediment echosounder (Atlas Hydrographics) represents a narrow beam sediment sub-bottom profiler. Two frequencies (18 kHz and 22 kHz) are emitted from hull-mounted transducers. Due to the parametric effect a 4 kHz signal is generated in the water column within an emitting cone of ca. 4°, which results in a foot print with a diameter of 7% of the water depth.

The signal penetration depth strongly depends on the lithology, grain size and gas load. The received data are digitised and stored in SEG-Y and PS3 format. Data processing and visualisation has been carried out by means of the SENT software package developed at the

University of Bremen by Volkhard Spieß and co-workers. Processing mainly included noise suppression and clipping adjustments. Data examples are presented in the subsequent chapter 5.2.

Bathymetric measurements have been carried out mainly with the hull mounted EM122 swath sounder. A swath of 256 preformed beams is emitted periodically with signal frequencies of 12 kHz. The usable foot print of a single emitted swath perpendicular to the ship's heading has a width of more than three times of the water depth. In areas shallower than approx. 300 m bathymetric measurements were carried out by the EM710 swath sounder in order to get a higher resolution and to prevent system failures. The EM710 is operating with a signal frequency of 70-100 kHz.

5.2 Sediments: Sampling, Logging, Facies

5.2.1. Piston Coring

Deployment

During research cruise M94 with RV METEOR, 7 piston corers (PC) with core barrel lengths between 10 and 20 m were run (Table 5.2.1.1). Although seafloor sediments were extremely hard to penetrate, and ship manoeuvering was difficult due to up to 4 kn current speed, six deployments were successful, resulting in a total core recovery of 36.61 m, including 1.28 m core length recovered by the pilot corer (TC) triggering the piston corer (Figure 5.2.1.1). One deployment was not successful.

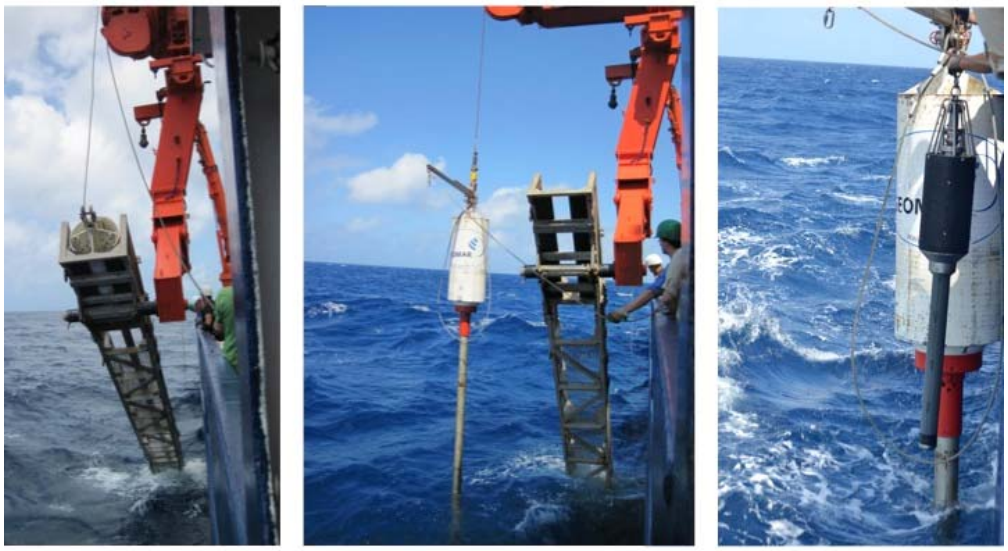

Fig. 5.2.1.1 Deployment and operation of the GEOMAR piston corer.

Coring concentrated on three regions:

- ***Working area 1 (Yucatan Strait):*** 5 PC deployments (barrel lengths 10-20 m) recovered sediment cores of ~2.7 m.
- ***Working area 2 (southern Campeche Bank):*** 2 PC (barrel lengths 10-20 m) recovered core lengths of 6.3 m.
- ***Working area 3 (northern Campeche Bank):*** 3 PC deployments (barrel lengths 10-20 m) recovered on average 5.9 m long sediment records.

The gear types and length of the coring devices were chosen based on detailed acoustic sediment mapping performed with the ATLAS PARASOUND echosounding system and the reflection

seismics of Hamburg University prior to coring. Acoustic patterns such as the strength of characteristic reflectors, their spacing, and the total sub-bottom penetration were taken into account.

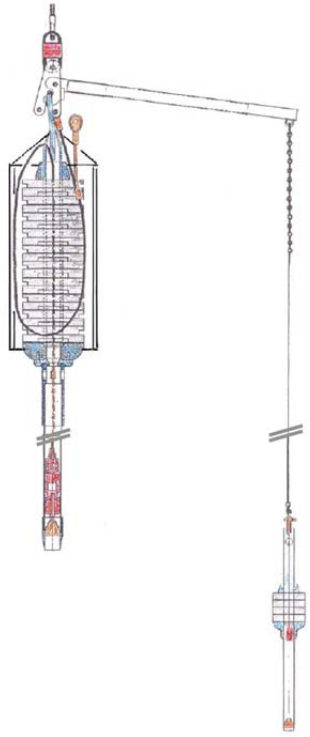

Fig. 5.2.1.2 Schematic diagram of the GEOMAR split-piston corer from Fa. Marinetechnik Kawohl.

Table 5.2.1.1. Sediment coring locations during M94.

Station	Device	Location	Date	Latitude N		Longitude W		Water	Pipe	Recovery	Section	Pilot
No.				°	dec.min.	°	dec.min.	depth (m)	length (cm)	(cm)	number	(cm)
M94-473	PC	Yucatan Strait	03/18/ 2013	21	44.646	86	14.163	933	2000	273	3	94
M94-475	PC	Yucatan Strait	03/18/ 2013	21	46.277	86	16.084	767	1000	280	3	15
M94-478	PC	southern Campeche Bank	03/19/ 2013	22	43.059	86	26.544	749.3	1000	631	7	0
M94-480	PC	deep northern Campeche Bank	03/21/ 2013	23	48.141	87	0.868	730	1500	1217	13	11
M94-481	PC	shallow northern Campeche Bank	03/21/ 2013	23	39.997	87	7.284	520.8	1000	251	3	0
M94-482	PC	mid-depth northern Campeche Bank	03/21/ 2013	23	49.155	87	7.752	629.8	2000	881	9	0-8
M94-484	PC	southern Campeche Bank	03/22/ 2013	22	41.635	86	22.339	909	2000	0	0	0

The GEOMAR piston corer with split piston developed by Fa. Kawohl Marinetechnik (marinetech.-kawohl@tonline.de) was fitted with a core barrel of max. 20 m in length (in 5 m increments). The core diameter is 12.5 cm, and the weight barrel is ~3.5 tons (Figure 5.2.1.2). On RV METEOR, the piston corer was deployed with an 18 mm steel cable attached to the ship´s deep-sea winch. The piston corer was lowered with an average speed of 1.0 m/s to ~50 m above seafloor and stopped for ~3 minutes to level out. Subsequently, it was lowered with 0.3

m/s until the pilot trigger core hit the seafloor. Contact with the seafloor was monitored through cable tension. When the pilot core reached the seafloor, the piston corer was released, free falling by ~5 m before reaching the seafloor, and penetrating into the sediments. The device remained at the seafloor for ~30 seconds after piston release in order to allow for deep penetration, then pulled out with a speed of 0.1 m/s. Once out of the sediment indicated by cable tension relief, the piston core was heaved up with a speed of 1.0 m/s.

Core handling

The 5m-PVC-core liners of the piston cores were oriented, labeled, and commonly cut into 1 m sections. Cores were subsequently opened for ongoing on-board processing (Table 5.2.1.1). Each 1 m-section was split into working and archive halves. The sediment surface was cleaned and smoothed before core photos were taken, and lithological description started (see Appendix 1). Color reflectance measurements were accomplished from the archive half. The archive and working halves were usually packed into plastic D-tubes and stored at ~4°C in the RV METEOR cooling store, and later transferred into the reefer for home transport. Only for selected cores, the working halves were sampled, providing sediment material for the various working groups (Fig. 5.2.1.3).

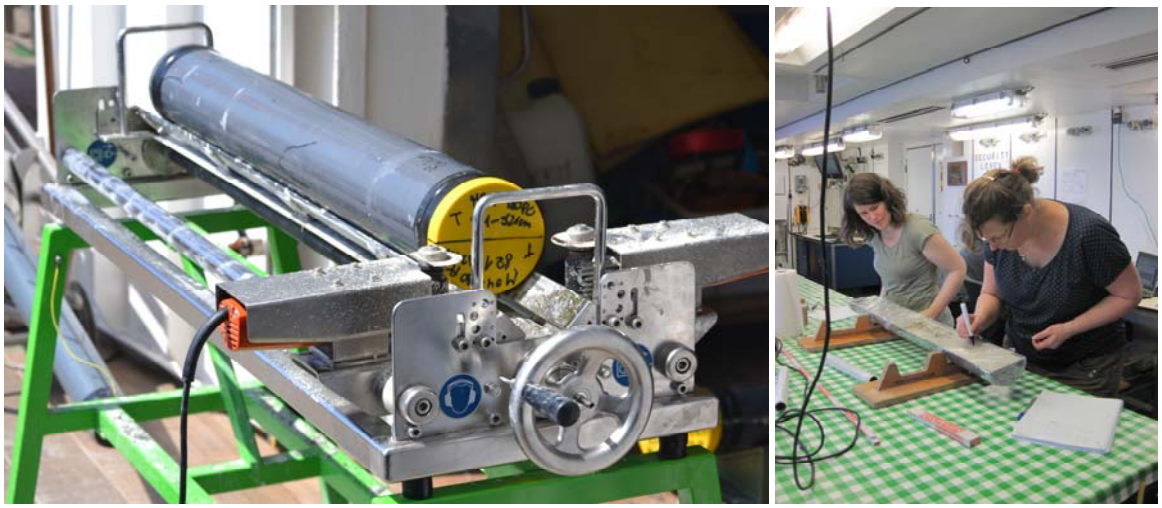

Fig. 5.2.1.3 Left: Opening of PVC-core liner with the liner saw (Fa. Kawohl Marinetechnik). Right: Sampling of sediment.

Sediment core liners and D-Tubes contain the following information (Figure 5.2.1.4):

- Core number (e.g., M94-473 PC),
- "A" for archive half, "W" for working half,
- Arrow pointing to base with depths of section top and base,
- Top and base of each section is marked with "Top" and "Base/Bottom", respectively, and the continuous depth alongside the core.

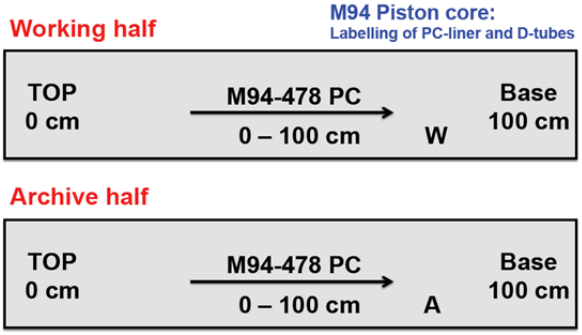

Fig. 5.2.1.4 Labelling of core liners and D-tubes.

The sediment core descriptions (Appendix 1) are presented as lithology strip logs and summarize logging data, core photography, and onboard visual inspections of each core. All graphical core descriptions were documented with the software package AppleCORE version 10.1t (by Mike Ranger, 2011), using a lithology custom file containing patterns following the standard IODP/ODP sediment classification scheme, a modified version of the lithologic classification of Mazzullo et al. (1988). Sediments were named on the basis of composition and texture, using a principal name together with major and minor modifiers (see Chapter 5.2.3). Sediment core descriptions were performed on the working half. According to the classification of Mazzullo et al. (1988), sediments encountered during M94 are fine to coarse grained sediments consisting predominantly of biogenic particles. Sediment names consist of a principal name related to the major biogenic component and the degree of compaction.

During expedition M94, we recovered unconsolidated calcareous biogenic sediments (generally "ooze", and if dominated by foraminifera, "sand"). For biogenic sediments with a larger silty/clayey component, we here used the principal name describing the texture (shale/mudstone). In total, we identified four major lithologies in the cores recovered on the M94 cruise: a foraminiferal ooze, a foram-rich silty sand, a foram-rich shale/mudstone and a fine-grained coccolith ooze.

Further information presented in the lithology strip logs includes the location and nature of sedimentary structures, the occurrence of fossils, ichnofossils, the degree of bioturbation, and accessories (such as burrows, laminae, shell fragments, manganese mottles, volcanic fragments, etc.), and articifial core disturbance.

As the color measurements taken with the Minolta spectrophotometer are reliable, we included the Y (D65)-records into the lithology strip logs. Core sections were photographed using a digital camera (Nikon D3100). The single images were added to the lithology strip logs, and also arranged for each core and presented in the Appendix 2.

Sampling scheme of sediment cores

The 1 m-long half segments of selected sediment cores were sampled according to the following scheme. Due to disturbance during coring operations, some segments were not completely filled with sediment. These segments were not sampled, as XRF-scanning will be performed first in the home lab. Sampling of selected sediment cores was done cm-wise. The samples were taken in whole slices and were placed in plastic bags (Whirl-Pak). Samples were stored at 4°C. Additionally, every ~50 cm samples were taken for physical property analyses and biostratigraphy in syringes. Samples were provided to Matthew Schmidt (AMU, USA) and Maria Alvarez Garcia (CEUNIVO, Mexico).

5.2.2 Shipboard Core Logging: MINOLTA Color-Scanning

The MINOLTA CM-600d hand-held spectrophotometer was used for color scanning (Figure 5.2.2.1). The measurement of the light reflectance was done on the sediment surfaces of opened core sections. Before placing the Minolta device on the sediment core, the sediment surface was covered with clean and clear polyethylene foil and smoothed in order to avoid the inclusion of air bubbles at the foil-sediment interface. The spectrophotometer was calibrated to avoid any variation in color measurements due to the environmental (temperature, humidity, background light) and industrial variations. Before the measurement of each core segment, the device was calibrated for black color once using "zero-calibration" as well as for white color reflections. The spectrum of the reflected light was measured by a multi-segment light sensor over a wavelength spectrum from 400 to 700 nm at a 10 nm pitch. The variation in the illumination from the device pulsed xenon arc lamp was automatically compensated by a double-beam feedback system.

Routinely, the reflection data and standard color measurements were taken at 1 cm steps, and were automatically recorded and processed by the software MINOLTA SpectraMagic v.2.3. The data are displayed in the Y(D65), L*, a* and b* CIELAB color coordinates. The L*-value

represents brightness and can be directly correlated to grey value measurements, whereas Y(D65) represents the lightness on a linear scale and L* on a non-linear scale. The a*-values indicate the relationship between green and magenta and the b*-value reflects blue/yellow colors. The color scans of each core are displayed in the Appendix 3, while the Y(D65)-records are also shown in the lithology logs (Appendix 1).

Fig. 5.2.2.1 Color scanning the M94 sediment cores.

5.2.3 Sediment Facies

Preliminary interpretations of the sediment facies are based on sedimentological and physical properties, as well as color-scan data and visual inspection of the cores. Sediment cores were retrieved from the Yucatan Straits and both the southern and northern Campeche Bank in the southern Gulf of Mexico (Fig. 3.1.1). We identified four major lithologies in the cores recovered on the M94 cruise:

Foraminiferal ooze

The coarse-grained foraminiferal sand composed of >30% foram shells is defined as foraminiferal ooze. The color ranges from beige to light and medium gray. It contains abundant pteropods and the planktonic foraminiferal specied *Globigerinoides ruber* pink. The lightness Y(D65) data indicate very high values. This sediment type is encountered in areas we interprete to have higher bottom-water currents, typical of the Yucatan Straits, and it was difficult to recover with our piston-coring system.

Foraminiferal-rich silty sand

The foraminifer-rich silty sand entirely consists of well-preserved calcitic tests of planktonic foraminifera and silt-sized grains. It also contains abundant pteropods. The color varies from medium to light tan, and often contains distinct gray mottling probably caused by the presence of burrows. This sediment is strongly bioturbated. The lightness Y(D65) data vary from high to low in this sediment type, depending on the color. We had better success to recover this sediment type with our piston coring system.

Foram-rich shale/mudstone

The foram-rich shale/mudstone is a fine-grained, carbonate-rich silty clayey sediment containing abundant foraminifera and pteropods. Color varies from light to medium gray, often containing darker gray mottling. The sediment is strongly bioturbated and contains abundant horizontal burrows several cm thick. The lightness Y(D65) data are generally medium to high values. We had the best recovery with our piston corer in this sediment type, recovering more than 12 m in core M94-480 PC on Campeche Bank. We interprete this sediment type to reflect relatively high accumulation rates in a low-energy environment.

Coccolith ooze

The coccolith ooze is built up by fine-grained, carbonate-rich sediment thought to be composed mainly of calcareous nannofossils and silt-sized grains. The sediment contains abundant foraminifera. The lightness Y(D65) data indicate medium values. This sediment type is encountered downcore at about 2.5 m in both Yucatan Straits cores M94-473 and M94-475.

5.2.3.1 Yucatan Strait

Our previous studies in Yucatan Strait during M78 (Schönfeld et al., 2012) showed that Yucatan Strait sediments are characterized by coarse to middle carbonate sands, which pass into silty middle to fine sands below 380 m. $CaCO_3$-concentrations are commonly >80%. The uppermost sediment appears acoustically transparent in water depths <450 m, which is due to dominating, well-sorted and highly porous foraminiferal sands. The surface sediment commonly changes to silty clay below ~750 m depth, where the average flow of bottom currents is <10 cm/s (Sheinbaum et al., 2002).

Hübscher et al. (2010) published a 43-km-long and west–east striking seismic profile that covers a seafloor depth range of 50–1550 m from the western flank of the Yucatan Strait (Figure 5.2.3.1.1). At ~810-880 m water depth, a 1-km-wide sediment infilled depression separates less stratified deposits above from a well stratified sediment succession with subparallel internal reflections below. The lower sequence is interpreted to originate from southward flowing currents through Yucatan Strait, while the upper sequence is produced from northward flowing water masses. The boundary between both flow regimes coincides with the lower boundary of the Antarctic Intermediate Water (AAIW), as revealed by a CTD-profile in Yucatan Strait accomplished during M78 (Figure 3.2.2).

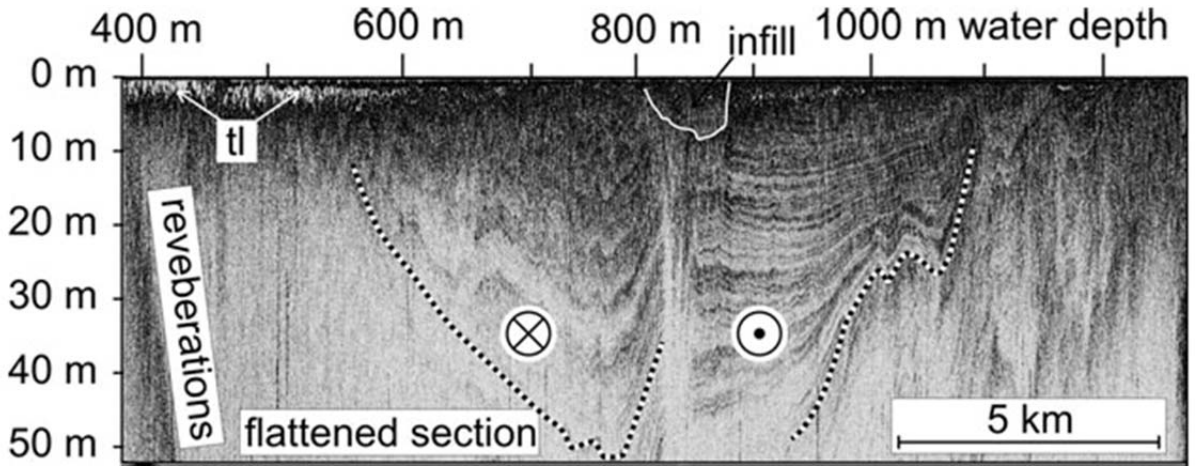

Fig. 5.2.3.1.1 Flattened PARASOUND section from the western side of Yucatan Strait taken during M78/1 (Hübscher et al., 2010). Circle with dot denotes southward flow, circle with cross denotes northward flow according to Sheinbaum et al. (2002). Note: tl = transparent layer of 2-4 m at top.

We retrieved two piston cores (plus pilot core) from above and below the abovementioned boundary from within the Antarctic Intermediate Water (M94-475, 767 m water depth) and from below (M94-473, 933 m water depth) (Figure 5.2.3.1.2). Although within different water masses, both sedimentary sequences are surprisingly similar pointing to equal depositional environments, with foraminiferal sand at the top grading into a fine, foraminifer-bearing calcareous ooze, separated by a thin but distinct brown silt/clay layer (Figure 5.2.3.1.3). The Minolta scanner data allow to closely correlated both records (Figure 5.2.3.1.3). We speculate that as the sediments are mainly composed of planktonic organisms reflecting surface conditions, the less abundant benthic microfossils may instead carry the signatures of the different intermediate to deep water masses.

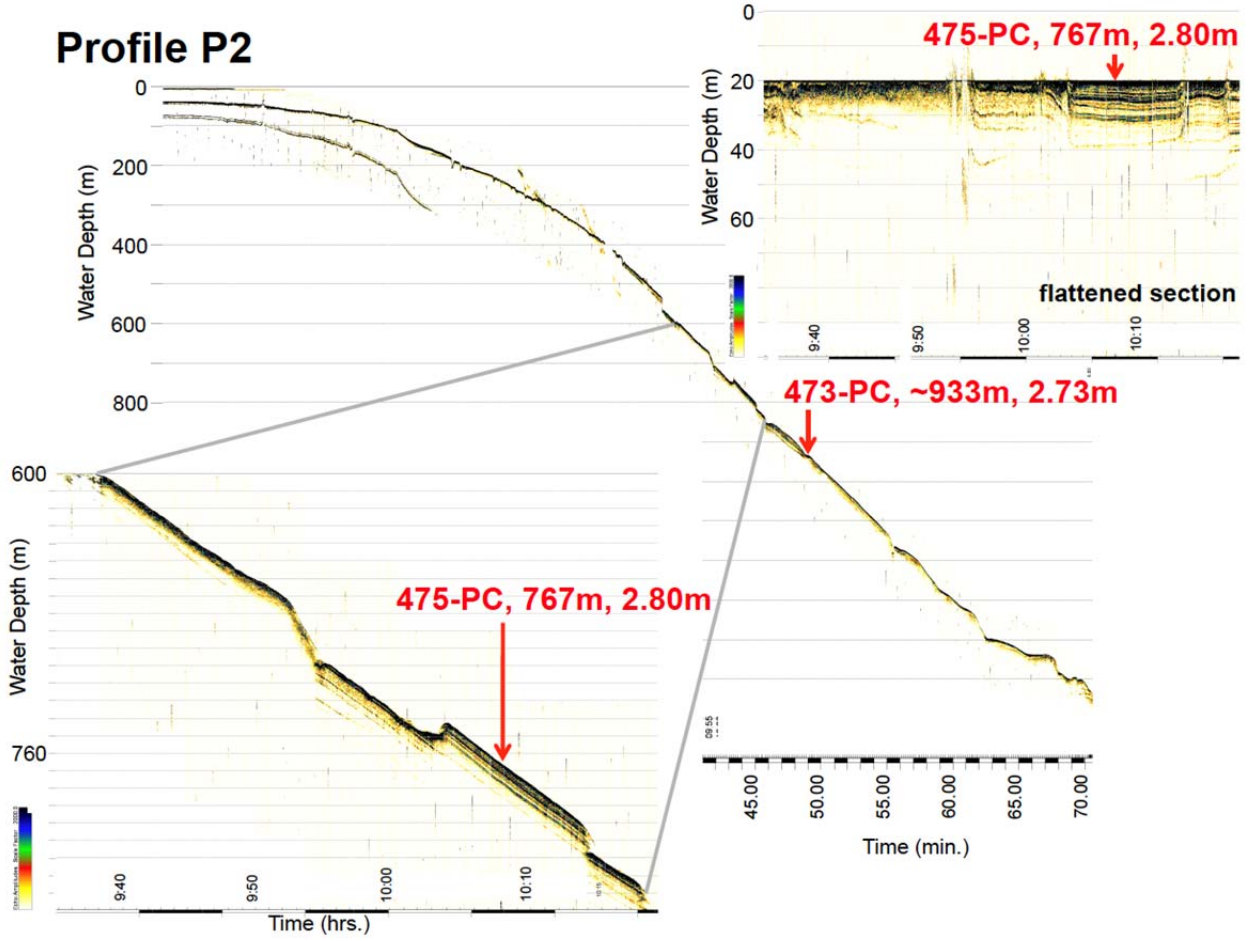

Fig. 5.2.3.1.2 West–east striking seismic profile (P2) that covers a seafloor depth range of ~50–1600 m from the western flank of the Yucatan Strait, accomplished during M94. Site locations of piston corers are indicated. Lower left inlet is the enhancements of the mid-depth part of the profile. Upper right inlet is the respective flattened section. For location see Fig. 5.3.2.1.

The Campeche Bank is characterized by coarse to middle foraminiferal ooze, which becomes finer at greater depth. Piston corer M94-478 PC was retrieved from ~750 m water depth (Figure 5.2.3.2.1), hence, from the core of the Antarctic Intermediate Water entering the Gulf of Mexico *via* Yucatan Strait. As expected, it consists of an intercalated sequence of foraminiferal ooze and silty foraminiferal sand. The core is undisturbed and of high quality for paleoceanographic studies. The MINOLTA Y(D65) data show pronounced amplitude variations downcore, most likely reflecting glacial/interglacial changes, similar to the M94-481 PC-record.

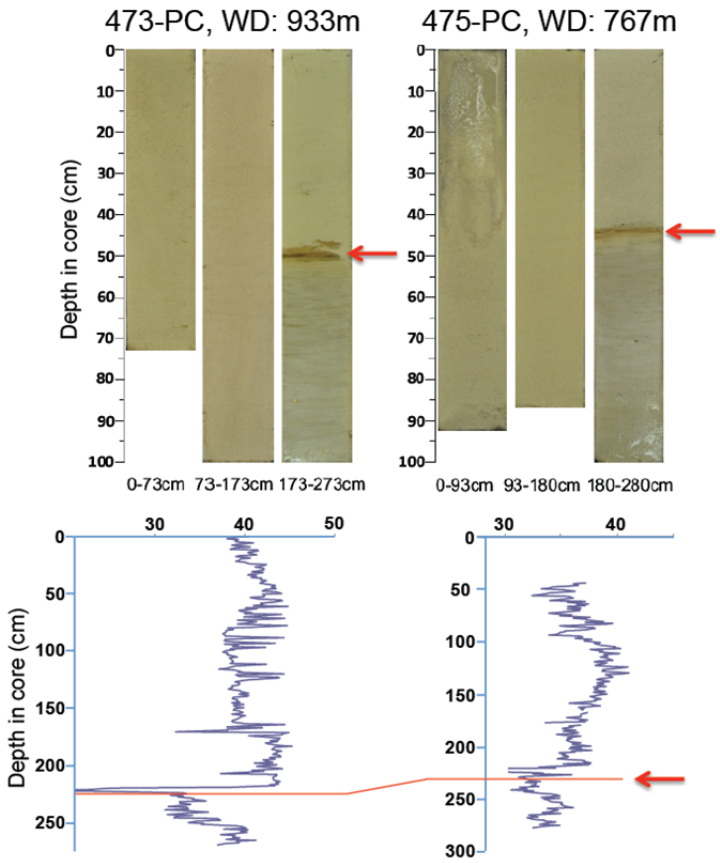

Fig. 5.2.3.1.3 Core images of piston cores M94-473 PC and M94-475 PC and the respective MINOLTA Y(D65) values vs. core depth. Although recovered from different water depths and current regimes, the sedimentlogy is similar. A prominent horizon is marked with a red arrow.

5.2.3.2 Southern Campeche Bank

Our second trial to retrieve a sediment core from the deeper southern Campeche Bank (station M94-484, 912 m water depth) unfortunately failed.

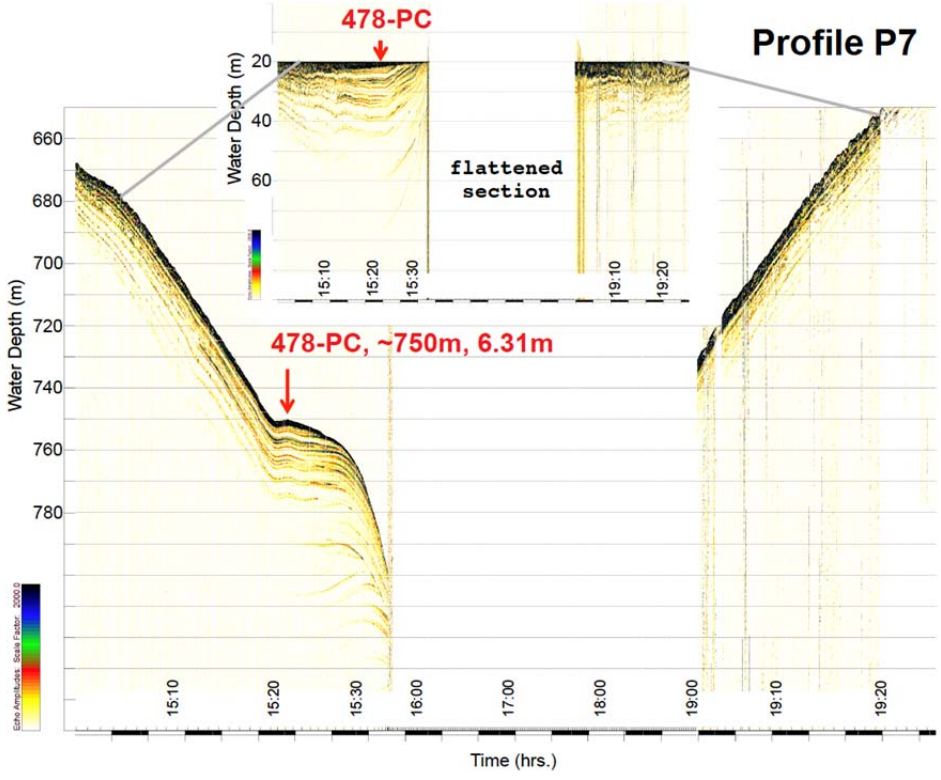

Fig. 5.2.3.2.1 West–east striking seismic profile (P7) that covers a seafloor depth range of ~670–800 m from the southern Campeche Bank, accomplished during M94. The location of piston corer M94-478 PC (~750 m water depth, ~6.3 m core recovery) is indicated. Upper inlet is the respective flattened section. For location see Fig. 5.3.2.1.

5.2.3.3 Northern Campeche Bank

Hübscher et al. (2010) published a seismic PARASOUND profile from the northern Campeche Bank (Figure 5.2.3.3.1), which revealed thick contourite drift bodies between ~600 m and 800 m water depth. The presence of distinct erosional unconformities within these drifts implies prominent re-organizations of the Yucatan Strait Throughflow pattern, the timing of which is yet unknown. The lower boundary of the contourite drift is defined by an escarpment, while above ~600m it is replaced by a mounded sediment complex. Here, the erosional unconformity raises to ~4 m below seafloor.

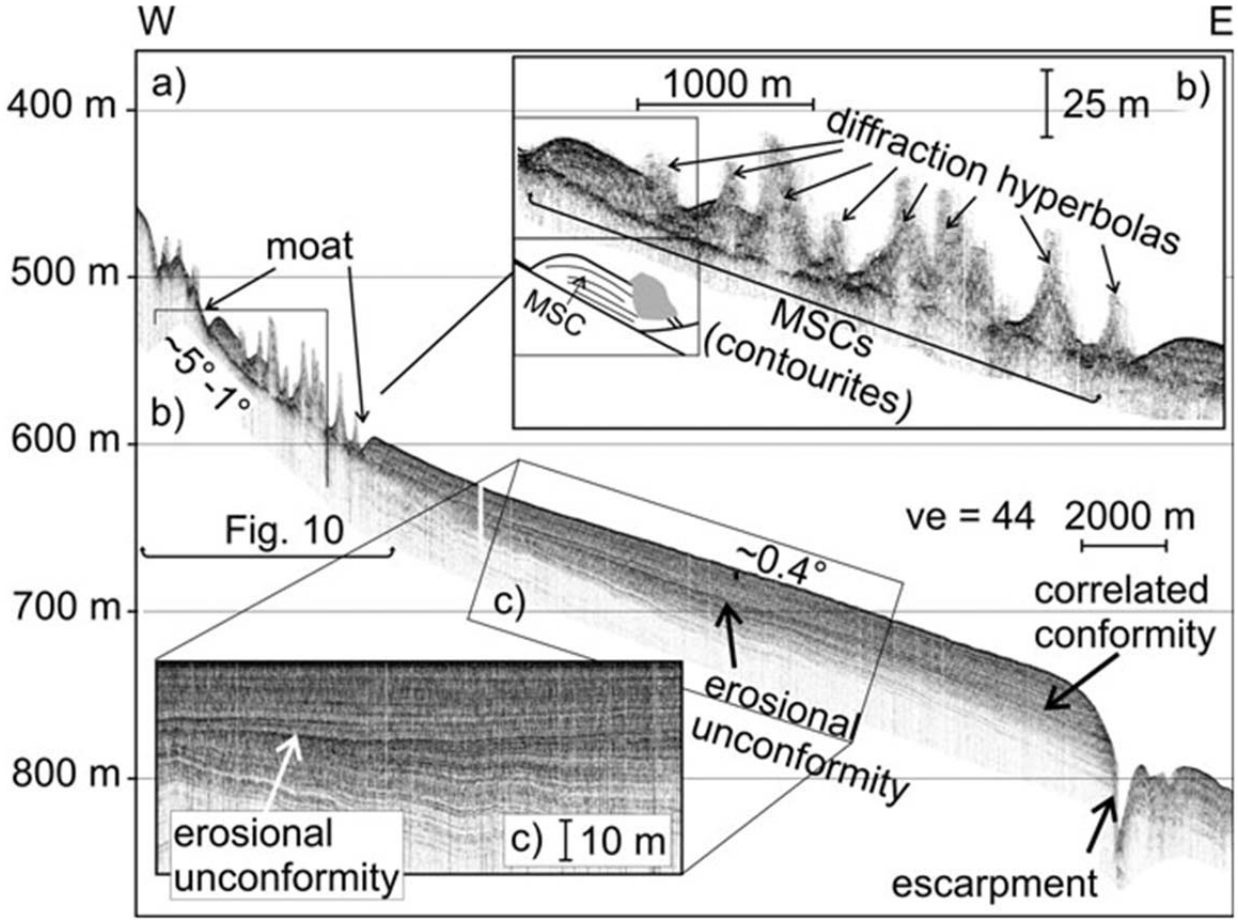

Fig. 5.2.3.3.1 PARASOUND section from the northeastern Campeche Bank from Hübscher et al. (2010). In water depths between 520 m and 600 m, a system of mounded sediment complexes (MSC) is present. Below and above a prominent escarpment, a layered sequence of sediments is present, with a correlated conformity in the lower part transforming into an erosional unconformity further upslope.

During M94, the drifts were surveyed more systematically by multi-channel SPARKER profiling, and three piston cores were recovered. Piston core M94-480 PC was recovered from intermediate depths (~730 m) from the northeastern Campeche Bank penetrating the layered sequence of sediments (Figure 5.2.3.3.2). Core recovery was ~12.2 m revealing undisturbed carbonate oozes of excellent quality (Appendix 2). The second piston core M94-482 PC (~7.8 m core recovery) was on the same transect at ~630 m water depth revealing the same sedimentary sequences as core M94-480 PC (Appendix 2), with a better preservation of the uppermost sediments.

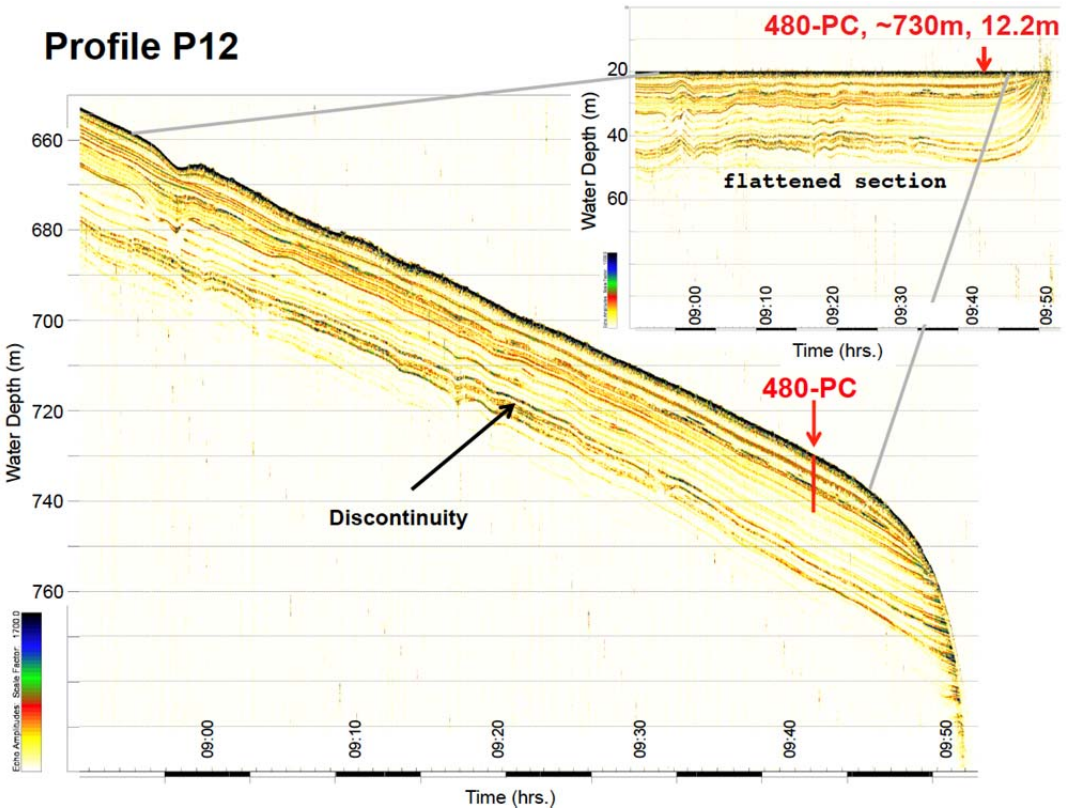

Fig. 5.2.3.3.2. West–east striking seismic profile (P12) that covers a seafloor depth range of ~650–800 m from the northern Campeche Bank, accomplished during M94. The locations of piston corer M94-480 PC (~730 m water depth, ~12.2 m core recovery) is indicated. Upper right inlet is the respective flattened section. For location see Fig. 5.3.2.1.

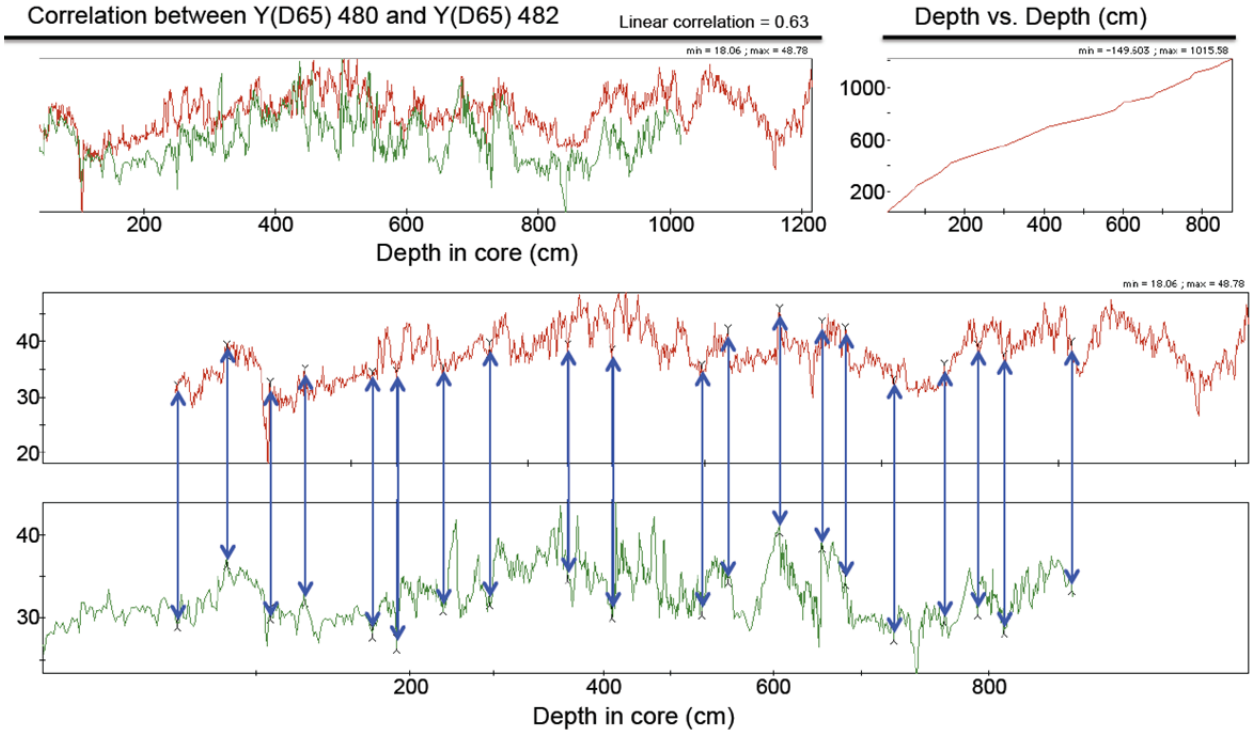

Fig. 5.2.3.3.3 Correlation of the MINOLTA Y(D65) values of cores M94-480 PC (~730 m water depth, ~12.2 m core recovery) and M94-482 PC (~630 m water depth, ~7.8 m core recovery) from the northeastern Campeche Bank. Correlation performed with AnalySeries 3.0 (PAILLARD et al., 1996). Lower diagram shows core M94-482 PC (green) related to reference record (M94-480 PC, red) using tie lines (vertical blue arrows). Upper left diagram shows tuning result with both cores on the same depth scale. Upper right diagram shows depth vs. depth diagram.

The tentative correlation of the M94-480 PC MINOLTA Y(D65) data towards the dated MD02-2575 sea surface temperature record from the northern Gulf of Mexico (Nürnberg et al., 2008) suggests that the 12 m long sediment core covers ~120.000 years, leading to a considerably high sedimentation rate of ~10 cm/kyr (Figure 5.2.3.3.3). The third piston corer M94-481 PC from the northern Campeche Bank transect is from ~521 m water depth within the mounded sediment complex (Figure 5.2.3.3.4). Although core recovery was only ~2.5 m, the core presumably reached the erosional unconformity first described by Hübscher et al. (2010) and subsequently mapped in more detail during M94. Core M94-481 PC consists of an intercalated sequence of light foraminiferal ooze and sand, and darker foram-rich shale/mudstone (Appendix 2), basically reflecting glacial/interglacial climatic changes. Below this sequence at ~2.3 m core depth, the lithology drastically changes into a very coarse-grained, diagenetically concreted sediment with sandsized grains cemented into even larger particles ranging from a few millimeter to several centimeter. Large brachiopods up to 2-3 cm in length are present. The contact to the upper sediment is sharp. We consider this sediment as clearly older and different than the overlying sediments, presumably separated by the erosional unconformity seen in the seismic data. Our attempt to derive a tentative age estimate for the erosional unconformity is based on the tuning of the MINOLTA Y(D65) data of core M94-481 PC towards the stable oxygen isotope reference record of Lisiecki and Raymo (2005), which has an accurate chronostratigraphy. The correlation is convincing (Figure 5.2.3.3.5) showing that the Holocene is most likely missing in core M94-481 PC. The intercalated sediment sequence reflects glacial/interglacial changes back to Marine Isotope Stage 11. The erosional unconformity dates to ~500 ka, while the diagenetically affected sediment below is clearly older, although of still unknown age.

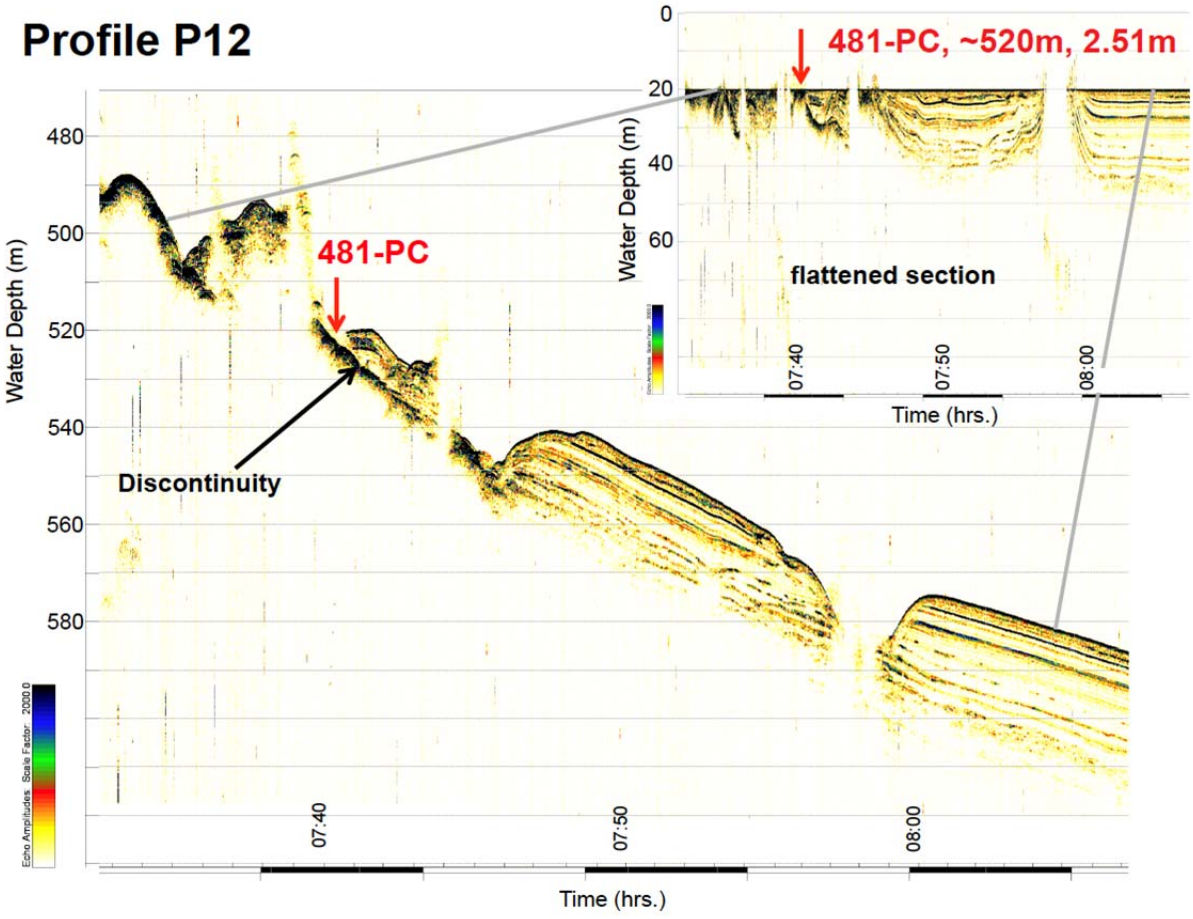

Fig. 5.2.3.3.4 SW–NE striking seismic profile (P12) that covers a seafloor depth range of ~470–590 m from the shallow northern Campeche Bank, accomplished during M94. The location of piston corer M94-481 PC (~520 m water depth, ~2.5 m core recovery) is indicated. Upper right inlet is the respective flattened section. For location see Fig. 5.3.2.1.

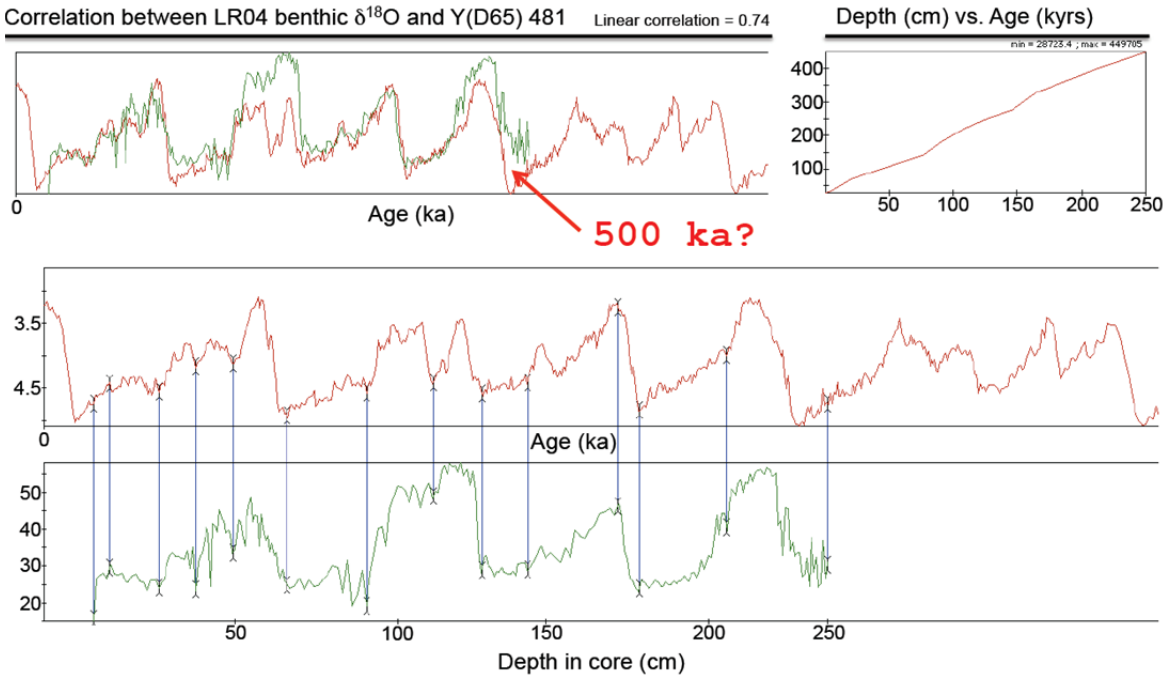

Fig. 5.2.3.3.5. Correlation of MINOLTA Y(D65) values (green) of core M94-481 PC (~521 m water depth, ~2.5 m core from the shallow northern Campeche Bank vs. the dated LR04 stable oxygen isotope reference record of LISIECKI and RAYMO (2005, red). The prominent lithological change, which is most likely the erosional unconformity, is tentatively dated to ~500 ka. Lower diagram shows reference record (LR04, red) related to core M94-481 PC (green) using tie lines (vertical lines). Upper light diagram shows tuning result with both cores on the LR04 age scale. Upper right diagram shows depth vs. age diagram.

According to our tentative stratigraphical approach, the formation of the unconformity and hence, the prominent change of the Loop Current system might be related to the end of the "Mid-Pleistocene Revolution". This profound change in the climate system at ~1 – 0.5 Ma describes the transition of earth´s climate from a more linear to a strongly non-linear climate system (e.g., Mudelsee and Stattegger, 1997) with the increase of the 100-kyr-cyclicity and the decrease in the 41-kyr-cycle amplitude.

5.3 Multi-Channel Seismics

5.3.1 Seismic Equipment

Seismic signals were generated by means of two clustered GI-Guns towed in a depth of appr. 2.5 m. The volume of each GI-Gun was 45 cin for the generator with a 105 cin injector volume. The operation mode was "true GI mode". The GI-Guns were synchronized by the SureShot trigger system, which displays the source signal of each airgun.

The data from the analog streamer (16 channels, 100 m active length) were recorded by the R48 StrataView seismograph, which includes a PC based A/D converter with pre-amplification and anti-alias filtering options. The dynamic range depends on sample rate, but it is always higher than 110 db. The CNT-1 controller PC performs storing, quality control (QC), and online plotting on the connected laser printer. Demultiplexed data were stored on RAID hard-drives and later on stored on LTO tapes. Quality control capabilities include several data display windows, which are shot window, gather plot, trigger window, noise window, and tape window. We generally chose a sample rate of 1 ms and a recording length of 2.5 s. A recording delay was adjusted to the water depth. For the impedance matching between the analog streamer and the seismograph we used a charge amplifier. Data recorded with this streamer were used for a rapid onboard processing and they serve as a backup in case the digital streamer fails.

In order to adapt the daily working plan to our findings, we created time-migrated brutestacks during the survey. Each brute-stack was finalized approximately 1 hour after finishing

acquisition of the specific profile. Processing has been carried out by using Seismic Unix. After converting the data from SEG-Y to SU format data where filtered using 10 Hz, 20 Hz, 200 Hz and 300 Hz as filter frequencies. In order to perform geo-referenced binning of the data, a navigation-file including the ship's position (latitude and longitude) for every 10 seconds was generated. The shot times were extracted from the trace headers and the shot positions were calculated by linear interpolation of the navigation data as well as taking the distance between GPS-antenna and gun-array into account. Assuming the streamer to be linear, the channel positions were calculated by knowledge of the channel-spacing and the initial offset, which has been estimated using the direct arrivals at the near offset channel. Subsequently, bins were calculated with a distance of 6.25 m and a binning radius of 12.5 m. For each line a brute-stack using a nmo-velocity of 1500 m/s was created. These brute-stacks were roughly migrated in the T-K domain with a constant interval velocity of 1500 m/s. Finally, the migrated sections were reconverted to SEG-Y-format in order to upload the geo-referenced dataset to an interpretation system for further analysis.

5.3.2 Data and Expected Results

The cruise track and seismic profile layout (Fig. 5.3.2.1) reflect the trade-off between scientific demands and time efficiency. Since sediment and water sampling was carried out during day light seismic profiling was bounded to the dark hours. All together 14 geophysical profiles have been collected. While hydroacoustic data (Parasound and multi-beam) were recorded continuously, seismic data were collected along 8 of them. 7 profiles strike perpendicular to the bathymetric contour (profiles 1, 2, 9c, 10, 11, 12, 14) and 1 runs contour parallel.

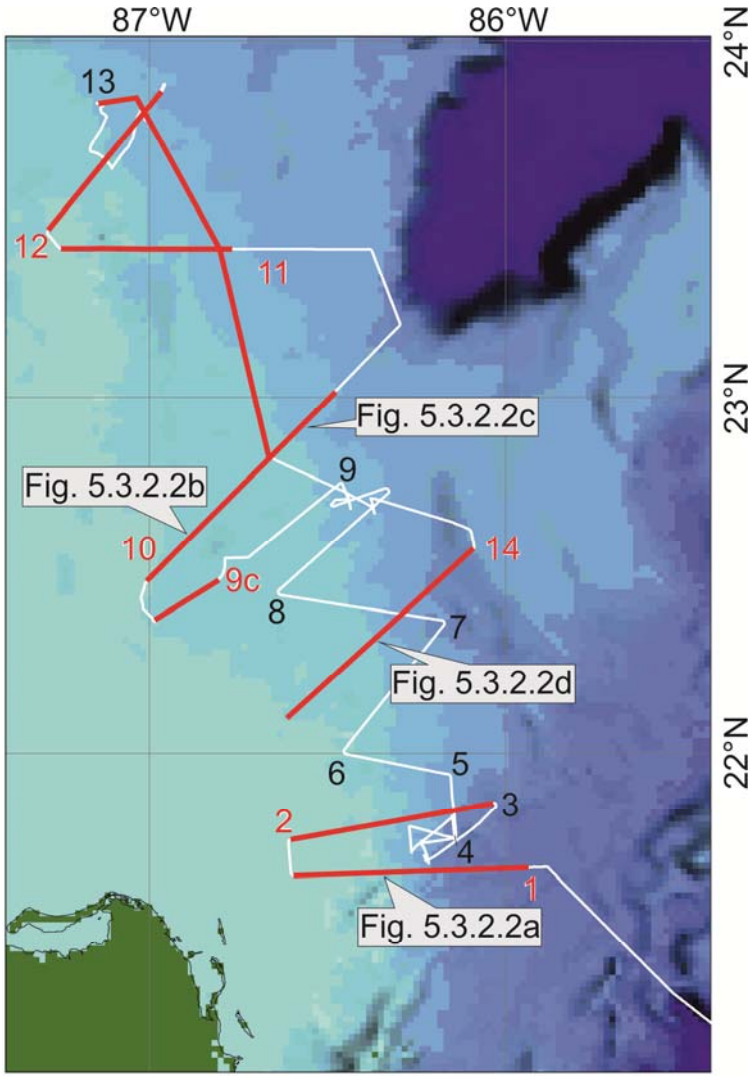

Fig. 5.3.2.1 Basemap showing M94 ship's track (white line) and multi-channel seismic profiles (red line). Numbers (red: seismics; black: Parasound & EM122) indicate profile numbers and are positioned on the beginning of the profile.

We observed four stratigraphic sequences on the eastern Campeche Bank (Fig. 5.3.2.2a). The lower two are aggrading, the third is prograding and it downlaps top sequence II. Its upper boundary reveals erosional truncation between 200 and 400 m depth (Fig. 5.3.2.2b). These lower three sequences cover the entire slop. Sequence IV shows topset aggradation down to 75 m depth and forest progradation down to 220 m. The clinoforms downlap the upper erosional unconformity of sequence III. We can just speculate that the sequence stratigraphy reflects onset and intensification of the Loop Current as part of the Gulfstream system and later paleoceanographic variations like the Mid-Pleistocene Transition.

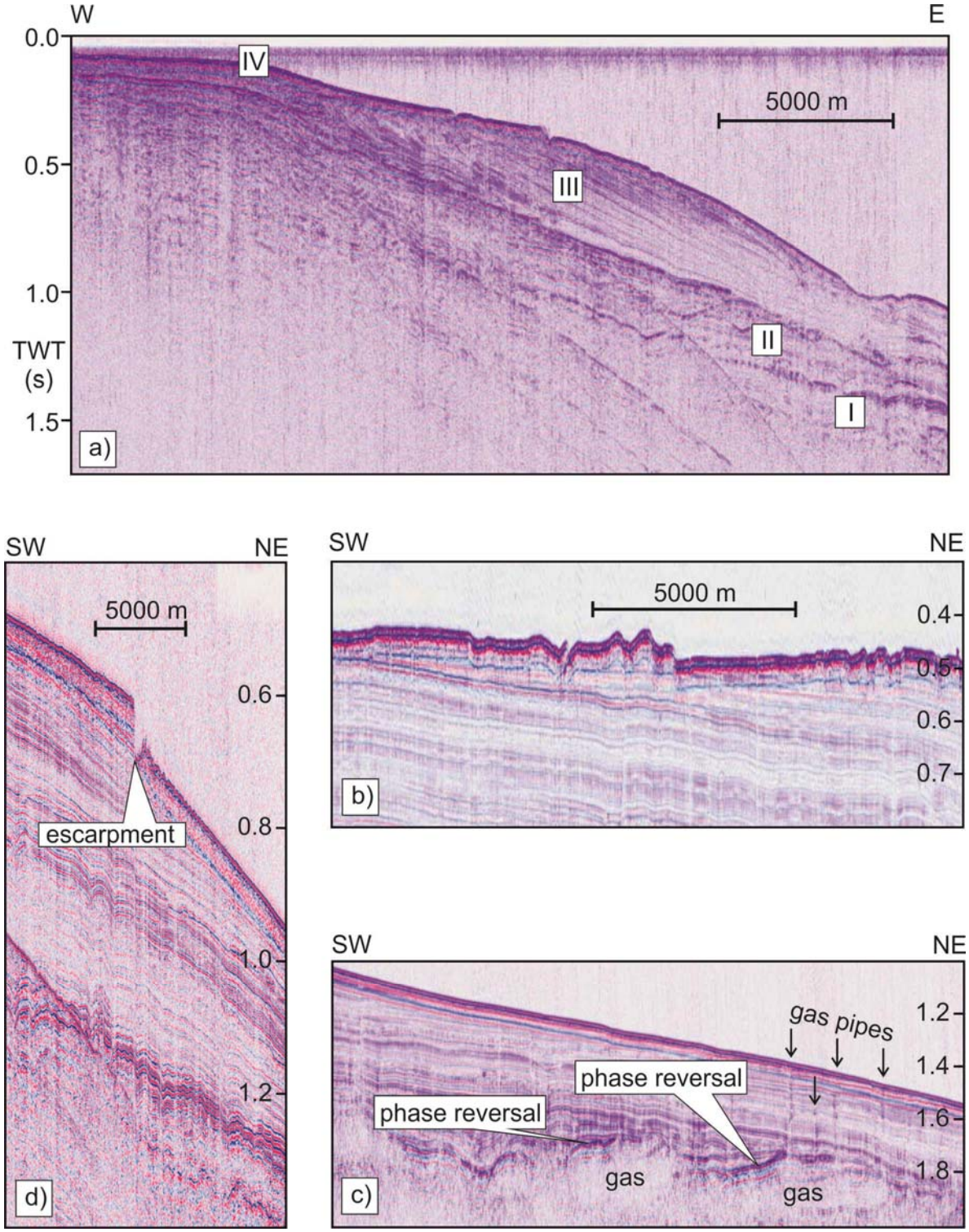

Fig. 5.3.2.2. Seismic sections, for locations see Fig. 5.3.2.1. See text for discussion.

Phase reversed reflection of high amplitude are present at the lower slope within sequences I and II, which we interpret as upper boundaries of gas charged sediments. This is corroborated by vertical pipes with strong reflection patches which are typical of vertical gas migration along pipes (Fig. 5.3.2.2c). A quite peculiar observation is the presence of arcuate escarpments and associated graben on the upper slope (Fig. 5.3.2.2d). Due to the coarse data grid the lateral along slope extension is unknown. The youngest unit of some 10 m thickness which is present upslope of the escarpment is missing downslope of it. Presence and evolution of these escarpments and graben is unexplained yet, the absence of the upper unit downslope of the escarpment could be explained by gravity gliding above a concordant decollement.

5.4. Water Column Sampling

The aim of the study is to investigate the habitat of recent living planktonic foraminifera and to analyze stable isotopes and trace metals of the tests in relation to the ambient seawater conditions in the Yucatan Strait. Therefore, living planktonic foraminifera were collected with an Apstein net from different water depths. Near surface plankton samples and water samples were taken by using the ship´s pump and hydrographic measurements were recorded with the shipboard thermosalinograph during the cruise M94.

5.4.1. Plankton Net

The Apstein net (Figure 5.4.1.1) was deployed to collect planktonic foraminifera at the station M94-474 in the Yucatan Strait (Table 5.4.1.1). The net was taken in different water depths of the uppermost water column: 100-60 m, 60-40 m, 40-20 m and 20-0 m. The net had a mesh size of 100 µm and an aperture of 17 cm diameter. It was heaved from 60-100 m two times and from the upper part three times. Before the final hauling a trigger weight was attached to the rope, which released the shutter closing the entry of the net. The net was washed with seawater on board and sampled into vials, and filled with ethanol.

First results show that the foraminiferal assemblage of the net samples was mainly composed of tropical species as *Globigerinoides sacculifer*, *Globigerinoides ruber* pink, *Globorotalia ungulata*, *Neogloboquadrina dutertrei*, *Globigerinita glutinata, Hastigerina pelagica* and *Orbulina universa* (Figure 5.4.1.2).

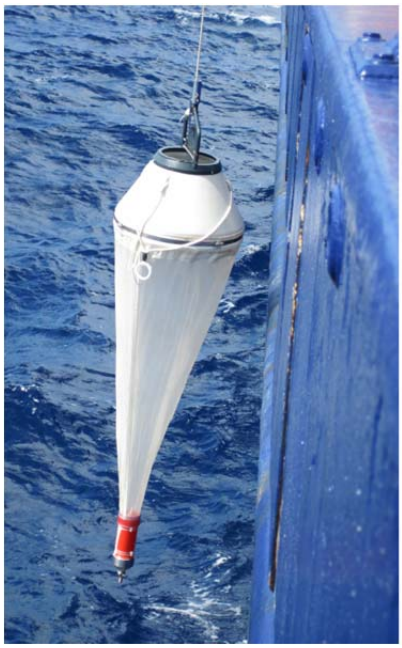

Fig. 5.4.1.1. The Apstein net deployed during M94..

Fig. 5.4.1.2. Living *Orbulina universa* from the Apstein Net sample M94-474 in 20-40 m water depth.

Table 5.4.1.1. Sampling depth, date and time, coordinates and water volume of the Apstein net M94-474.

Station Number	Sampling depth (m)	Date	Time UTC	Latitude N	Longitude W	Water volume (m^3)
M94-474	60-100	18.03.2013	14:45	21°45.500	86°08.500	1,71
	40-60		15:20			1,29
	20-40		15:45			1,29
	0-20		16:30			1,29

5.4.2. Zooplankton Filtering and Water Sampling

Planktonic foraminifera and water samples in near surface water were collected in the working area by using the ship´s pump. The surface water was taken from 3.5 m water depth and filtered by a device which has been constructed at GEOMAR (Figure 5.4.2.1). The zooplankton filter is made of a PVC tube of 40 cm in length and 10 cm in diameter with a sieve of 63 µm mesh size inside the tube to collect the plankton. Additionally, the filtered water volume was measured by a water meter between the seawater-tap and the filter system. We filtered approximately 1.7 m^3 water which took 2.5 - 3 hours. The filtered plankton was washed with seawater and transferred into plastic vials with seawater and ethanol.

Fig. 5.4.2.1 The plankton filter system.

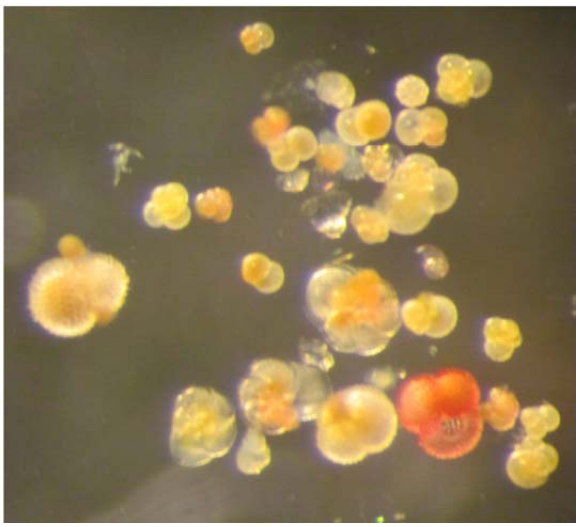

Fig. 5.4.2.2. The foraminiferal assemblage in the plankton filter sample with *G. sacculifer, G. glutinata, G. ruber* pink, and *G. menardii.*

Water samples were taken from the filtered water for stable isotope analysis ($\delta^{18}O$ and $\delta^{13}C$) and stored by 4° C. Salinity and temperature of the surface water was recorded by the thermosalinograph of the vessel during filtering.

A total of 12 plankton samples (Table 5.4.2.2) and 8 water samples (two duplicate samples of 100 ml each, Table 5.4.2.3) were taken in the working area and during transit time. The first results of the plankton filter samples showed a tropical fauna (Figure 5.4.2.2) with the dominant species *Globigerinoides sacculifer, Globigerinoides ruber* pink, *Globorotalia menardii/ungulata, Globigerinita glutinata, Bolivina variabilis*. According to Darling et al. (2009), the commonly benthic species *B. variabilis* may also live within the water column.

Table 5.4.2.2. Sample number, sampling depth, coordinates, date, time and filtered water volume of the Plankton Filter samples. S: Start of pump sampling, E: End of pump sampling.

Sample Number	Sampling depth (m)	Date	Time UTC	Latitude N	Longitude W	Water volume (m^3)
8	3,5	17.03.2013	13:02 (S) 15:59 (E)	20°41.880 (S) 21°03.981 (E)	84°50.264 (S) 85°12.184 (E)	1,988
9	3,5	17.03.2013	19:46 (S) 21:59 (N)	21°33.794 (S) 21°40.631 (N)	85°46.105 (S) 85°58.300 (N)	1,481
10	3,5	18.03.2013	13:05 (S) 15:45 (N)	21°51.250 (S) 21°42.129 (N)	86°01.610 (S) 86°13.353 (N)	1,77
11	3,5	19.03.2013	13:11 (S) 16:06 (E)	22°38.606 (S) 22°41.992 (E)	86°25.536 (S) 86°26.254 (E)	1,904
12	3,5	19.03.2013	19:57 (S) 22:54 (E)	22°40.087 (S) 22°29.666 (E)	86°34.460 (S) 86°47.897 (E)	1,921
13	3,5	20.03.2013	13:02 (S) 15:55 (E)	23°01.034 (S) 23°12.003 (E)	86°28.625 (S) 86°17.811 (E)	1,701
14	3,5	20.03.2013	19:51 (S) 22:43 (E)	23°24.925 (S) 23°24.952 (E)	86°29.832 (S) 86°45.971 (E)	1,743
15	3,5	21.03.2013	13:05 (S) 15:56 (E)	23°48.089 (S) 23°38.700 (E)	87°00.890 (S) 87°06.168 (E)	1,701
16	3,5	21.03.2013	20:36 (S) 22:51 (E)	23°49.012 (S) 23°49.713 (E)	87°07.965 (S) 87°07.147 (E)	1,047
17	3,5	22.03.2013	13:11 (S) 15:58 (E)	23°05.053 (S) 22°56.994 (E)	86°43.434 (S) 86°41.510 (E)	1,866
18	3,5	22.03.2013	19:19 (S) 21:50 (E)	22°49.636 (S) 22°40.433 (E)	86°39.286 (S) 86°22.059 (E)	1,766
19	3,5	23.03.2013	13:01 (S) 15:55 (E)	22°01.201 (S) 21°53.100 (E)	86°30.722 (S) 86°12.827 (E)	2,065

Table 5.4.2.3. Sample number, sampling depth, coordinates, date, time and taken water volume of the surface water samples for stable isotope analysis.

Sample Number	Sampling depth (m)	Date	Time UTC	Latitude N	Longitude W	Water volume (mL)
5	3.5	17.03.2013	14:37	20°53.795	84°59.268	2x 100
6	3.5	19.03.2013	14:30	22°43.053	86°24.771	2x 100
7	3.5	20.03.2013	14:51	23°07.970	86°21.840	2x 100
8	3.5	22.03.2013	14:41	23°00.684	86°42.388	2x 100

6 Ship's Meteorological Station

The vessel left the port of Balboa on the 12th of March at 9 p.m. and anchored offshore waiting for the passing of the Panama canal. On the next following day RV METEOR started to pass the Panama Canal which lasted into the 14th. While anchoring offshore and on the way of passing the canal, a high over Panama dominated the area with fine weather and a northerly winds about 4 Bft. The air temperature was hovering around 28 degrees. On the transit from the ITC to the work area a high to the north of the Gulf controlled the weather with northeast trade winds prevailing. While leaving the canal into the Caribbean water on the 14th the northerly winds strengthened to 5 to 6 Bft. A sea/swell of about 2.5 m was measured. The next following day the wind eased with a sea/swell decreasing to 1.5 m. Later in the period the high shifted to the east of Florida. On the 15th a weak cold front crossed the area with freshening winds to 6 to 7Bft. The sea reached a height of about 2.5 m. Waves spilled over the deck causing the on board work to be delayed. Overnight some weak showers passed. In the afternoon of the 17th the working area was reached. In the street of Yucatan the wind increased to 6 Bft. The high over the Gulf of Mexico weakened and shifted to the east. Southeasterly winds were experienced with only 4 to 5 Bft and a sea of about 1 to 1.5 m. Good working conditions prevailed in the area. On the 18th a low pressure system dominated over Mexico causing an increase of the pressure gradient. Therefore the south east wind increased to 5 to 6 Bft. During the night to the 20th in the vicinity of colder water close to 23N and 87W the wind increased to 6 Bft. Later until the 20th the high shifted to the east while the low pressure over Mexico weakened. Within a low pressure gradient good working conditions prevailed with a southeasterly wind about 4 Bft and a sea about 1 m. Later on the 20th a weak cold front crossed the area of RV METEOR. Some visible lightning

was evident in the distance. In the wake of the front the wind shifted north to northeast and increased to 5 to 6 Bft. The temperature of around 26 dropped to 22 degree. The sea height reached a level of 1.5 to 2 m. On the 22nd the weather pattern changed again. A large high pressure system was extending from the southwest of the US into the sea area to the northeast of Hispaniola. On contrast a large low pressure area over the western Gulf of Mexico causing the pressure gradient to increase. On the 22nd all wind and wave related work with the piston corer was terminated. The wind shifted to the southeast to south and reached strength of 6 to 7 Bft with a sea of about 3m. On the 23rd all work on the station was finished. RV METEOR cruised against wind and waves towards Jamaica. On the night to the 25th towards Cuba the southerly winds abated to 4 to 5 Bft with the sea only reaching a height of 1.5 m. On the 26th in the sea area close to Jamaica the wind shifted to the east and decreased to 3 to 4 Bft. In the afternoon of the 26th RV METEOR reached the port of Kingston in Jamaica.

7 Station List

Geophysical profiling:

Profile	Station	Start Lat. (N)	Long. (W)	End Lat (N)	Long. (W)	Length (km)	Shots	Type
1	M094/472	21°40.7’	85°56.8’	21°39.3’	86°35.5’	67	3868	S/H
2	M094/472	21°45.4’	86°36.1’	21°51.5’	86°02.3’	60	3954	S/H
3	M094/477	21°46.1’	86°08.4’	21°56.5’	86°09.9’	20		H
4	M094/477	21°56.5’	86°09.9’	22°01.0’	86°26.8’	32		H
5	M094/477	22°01.0’	86°26.8’	22°22.8’	86°13.5’	50		H
6	M094/477	22°22.8’	86°13.5’	22°26.7’	86°38.2’	50		H
7	M094/477	22°26.7’	86°38.2’	22°44.5’	86°19.8’	64		H
8	M094/477	22°44.5’	86°19.8’	22°42.1’	86°29.2’	35		H
9a	M094/479	22°45.4’	86°27.9’	22°28.7’	86°49.0’	17		H
9b	M094/479	22°28.7’	86°49.0’	22°22.9’	86°58.0’	19	1282	S/H
9c	M094/479	22°22.9’	86°88.0’	22°27.6’	87°00.9’	14		H
10	M094/479	22°28.5’	87°00.7’	23°11.9’	86°17.9’	110	6673	S/H
11	M094/479	23°24.9’	86°23.1’	23°25.0’	87°15.1’	89	4455	S/H
12	M094/479	23°27.7’	87°17.2’	23°51.3’	86°58.0’	55	3319	S/H
13	M094/483	23°49.7’	87°06.9’	22°49.6’	86°39.8’	129	9555	S/H
14	M094/485	22°34.4’	86°05.3’	22°04.9’	86°37.8’	79	4313	S/H

Type S: Multi-channel seismics + Parasound + Multibeam. Type H: Parasound + Multibeam.

Sampling Stations:

Station	Device	Lat .(N)	Long. (W)	Water depth (m)	Length of core (m)	Recovery (m)	Date (2013)	Time (UTC)
Yucatan Strait								
M094/473	Piston corer	21°44.646’	86°14.163’	933’	20	2.73	18.03.	17:57
M094/474	Plankton net	21°44.5’	86°08.5’	1536			18.03	14:45
M094/475	Piston corer	21°46.277’	86°16.084’	767	10	2.80	18.03	00:20
Southern Campeche Bank								
M094/478	Piston corer	22°43.059’	86°26.544’	749	10	6.31	19.03	18:04
M094/484	Piston corer	22°41.635’	86°22.339’	909	20	0	22.03	22:50
Northern Campeche Bank								
M094/480	Piston corer	23°48.141’	87°00.868’	730	15	12.17	21.03	13:21
M094/481	Piston corer	23°39.997’	87°07.284’	521	10	2.51	21.03	17:14
M094/482	Piston corer	23°49.155’	87°07.752’	630	20	8.81	21.03	

8 Data and Sample Storage and Availability

Station list, cruise track and bathymetric data obtained during RV METEOR cruise M94 are archived at the German Oceanographic Data Centre, Bundesamt für Seeschiffahrt und Hydrographie (BSH), Hamburg (http://www.seadata.bsh.de). Seismic and Hydroacoustic subsurface profiling data are curated at the Institut für Geophysik, Universität Hamburg (Christian Hübscher) and will be stored within the PANGAEA data base after publication. Swath mapping bathymetric data are archived at the German Oceanographic Data Centre, BSH. The hydrographic data obtained by the CTD cast are archived at PANGAEA database (http://www.pangaea.de). The descriptions of sediment cores are archived at PANGAEA together with light reflectivity data.

The samples taken on RV METEOR cruise M94 were distributed to the following principle investigators for initial analyses. Seawater and zooplankton samples (multinet and plankton pump) are analyzed by Anna Jentzen, Joachim Schönfeld, and Dirk Nürnberg at GEOMAR. Sediment cores are analyzed by Dirk Nürnberg, GEOMAR, Matthew Schmidt, A&M University, College Station, TX, USA,

Sediment cores are archived at the Lithothek Core Repository, GEOMAR, Kiel. Subsamples are available to the public upon request by January 2017.

9 Acknowledgements

We like to thank captain Michael Schneider, his officers and crew of RV METEOR for their support of our measurement programme and for creating a very friendly atmosphere on board. We further like to thank Wolfgang Mahrle (German Federal Foreign Office), Mr. Hubertus von Römer (German Embassy Mexico City) and Mr. Ansgar Sittman (German EmbassyWashington) for their great support during the diplomatic clearance. The ship time of RV METEOR was provided by the Deutsche Forschungsgemeinschaft (DFG).

10 References

Bard, E., Rostek, F., Turon, J.-L., Gendreau, S. (2000) Hydrological impact of Heinrich Events in the subtropical northeast Atlantic. Science 289, 1321-1324.

Berger, W.H., Wefer, G. (1996) Expeditions into the past: Paleoceanographic studies in the South Atlantic, in The South Atlantic: Present and Past Circulation, edited by G. Wefer et al., pp. 363–410, Springer, New York.

Berggren, W.A., Hollister, C.D. (1974) Paleogeography, paleobiogeography, and the history of circulation of the Atlantic Ocean. In Studies in Paleoceanography, edited by W. W. Hay, Spec. Publ. Soc. Econ. Paleontol. Mineral. 20, 126–186.

Blunier, T., Chappellaz, J., Schwander, J., Dällenbach, A., Stauffer, B., Stocker, T.F., Raynaud, D., Jouzel, J., Clausen, C.U. and Johnson, S.J. (1998) Asynchrony of Antarctic and Greenland climate change during the last glacial period. Nature, 391: 739-743.

Broecker, W.S., Denton, G.H. (1989) The role of ocean-atmosphere reorganizations in glacial cycles. Geochim. Cosmochim. Acta 53, 2465– 2501.

Bunge L., Ochoa, J., Badan, A., Candela, J., J. Sheinbaum (2002) Deep flows in the Yucatan Channel and their relation to changes in the Loop Current extension. J. Geophys. Res. 107 (C12), 3233, doi:10.1029/2001JC001256.

Darling, K.F., Thomas, E., Kasemann, S.A., Seears, H.A., Smart, C.W., and Wade, C.M. (2009) Surviving mass extinction by bridging the benthic/planktic divide. Proc. Natl. Acad. Sci. USA, 106: 12629-12633.

Driscoll, N.W., Haug, G.H. (1998) A short circuit in the thermohaline circulation: A cause for Northern Hemisphere glaciation? Science 282, 436– 438.

Ezer, T., Oey, L.-Y., Lee, H.-C., Sturges, W. (2003) The variability of currents in the Yucatan Channel: Analysis of results from a numerical ocean model. Journal of Geophysical Research 108, 3012.

Ganopolski, A., Rahmstorf, S., Petoukhov, V., Claussen, M. (1998) Simulation of modern and glacial climates with a coupled global model of intermediate complexity. Nature 391, 351-356.

Haddad, G.A., Droxler, A.W. (1996) Metastable $CaCO_3$ dissolution at intermediate water depths of the Caribbean and western North Atlantic: Implications for intermediate water circulation during the past 200,000 years. Paleoceanography 11, 701– 716.

Haug, G.H., Tiedemann, R. (1998) Effect of the formation of the Isthmus of Panama on Atlantic Ocean thermohaline circulation. Nature 393, 673–676.

Haug, G.H., Tiedemann, R., Zahn, R., Ravelo, A.C. (2001) Role of Panama uplift on oceanic freshwater balance. Geology 29, 207– 210.

Hübscher, Chr., Dullo. W.-C., Flögel., S., Titschak, J., Schönfeld, J. (2010) Contourite drift evolution and related coral growth in the eastern Gulf of Mexico and its gateways. Int J Earth Sci (Geol Rundsch) 99 (Suppl 1): 191–S206, DOI 10.1007/s00531-010-0558-6.

Johns, W.E., Townsend, T.L., Fratantoni, D.M., Wilson, W.D. (2002) On the Atlantic inflow to the Caribbean Sea. Deep Sea Research Part I: Oceanographic Research Papers 49, 211-243.

Jousaumme, S., Sadourny, R., Vignal, C. (1986) Origin of precipitating water in a numerical simulation of the July climate. Ocean Air Interact. 1, 43– 56.

Keigwin, L.D., Jones, G.A., Lehman, S.J. (1991) Deglacial meltwater discharge, North Atlantic deep circulation, and abrupt climate change. J. Geophys. Res. 96, 16.811-16.826.

Lisiecki, L.E., Raymo, M.E. (2005) A Pliocene–Pleistocene stack of 57 globally distributed benthic $\delta^{18}O$ records. Paleoceanography 20, PA1003. doi:10.1029/2004PA001071.

Mazzullo, J.M., Meyer, A., Kidd, R.B. (1988) New sediment classification scheme for the Ocean Drilling Program. In Mazzullo, J.M., Graham, A.G. (Eds.), Handbook for shipboard sedimentologists. ODP Tech. Note 8: 45–67. doi:10.2973/odp.tn.8.1988.

McManus, J., Francois, R., Gherardi, J.-M., Keigwin, L. D., Brown-Leger, S. (2004) Collapse and rapid resumption of Atlantic meridional circulation linked to deglacial climate changes. Nature 428, 834-837.

Mudelsee, M., Stattegger, K. (1997) Exploring the structure of the mid-Pleistocene revolution with advanced methods of time-series analysis. Geol. Rundsch. 86, 499—511.

Nürnberg, D., Ziegler, M., Karas, C., Tiedemann, R., Schmidt, M. W. (2008) Interacting Loop Current variability and Mississippi River discharge over the past 400 kyr. Earth and Planetary Science Letters 272, 278-289.

Oey, L.-Y. (2004) Vorticity flux through the Yucatan Channel and Loop Current variability in the Gulf of Mexico. Journal of Geophysical Research 109, C10004.

Oey, L.-Y., Lee, H.-C., Schmitz, W.J. (2003) Effects of wind and Caribbean eddies on the frequency of Loop Current eddy shedding: a numerical model study. Journal of Geophysical Research 108, 3324.

Paillard, D., Labeyrie, L., Yiou, P. (1996) Macintosh program performs time-series analysis, Eos Trans. AGU, 77: 379. An electronic supplement of this reference is available at: http://www.agu.org/eos_elec/96097e.html.

Pahnke, K., Goldstein, S., Hemming, S.R. (2008) Abrupt changes in Antarctic Intermediate Water circulation over the past 25,000 years. Nature Geoscience 1, doi:10.1038/ngeo360.

Pickard, G.L., Emery, W.J. (1982) Descriptive physical oceanography. Pergamon, Oxford, 249 pp.

Prange, M., Schulz, M. (2004) A coastal upwelling seesaw in the Atlantic Ocean as a result of the closure of the Central American Seaway. Geophys. Res. Lett. 31, L17207, doi:10.1029/2004GL020073.

Romanou, A., Chassignet, E. P., Sturges, W. (2004) Gulf of Mexico circulation within a high-resolution numerical simulation on the North Atlantic Ocean. Journal of Geophysical Research 109, C01003.

Rühlemann, C., Mulitza, S., Müller, P.J., Wefer, G., Zahn, R. (1999) Warming of the tropical Atlantic Ocean and slowdown of thermohaline circulation during the last deglaciation. Nature 402, 511– 514.

Rühlemann, C., Mulitza, S., Lohmann, G., Paul, A., Prange, M., Wefer, G. (2004) Intermediate depth warming in the tropical Atlantic related to weakened thermohaline circulation: Combining paleoclimate data and modeling results for the last deglaciation. Paleoceanography, 19, PA1025, doi:10.1029/2003PA000948.

Schmidt, M.W., Vautravers, M.J., Spero, H.J. (2006) Western Caribbean sea surface temperatures during the late Quaternary. Geochemistry, Geophysics, Geosystems 7, Q02P10.

Schönfeld, J., Seifert, R., Krastel-Gudegast, S., Wefer, G. (2009) Forschungsschiff / Research Vessel Meteor Reise Nr. 78 / Cruise No.78 21. 2. 2009 – 6. 7. 2009 "Caribbean palaeoceanography, energy and mass transfer on the Mid-Atlantic Ridge, sediment transport off Uruguay and Argentinia" Forschungsschiff Meteor: Reise Nr. M78 . Leitstelle Dt. Forschungsschiffe, Hamburg, Germany, 49 pp.

Schönfeld, J., Bahr, A., Bannert, B., Bayer, A. S., Bayer, M., Beer, C., Blanz, T., Dullo, W. C., Flögel, S., Garlichs, T., Haley, B. A., Hübscher, C., Joseph, N., Kucera, M., Langenbacher, J., Nürnberg, D., Ochsenhirt, W. T., Petersen, A., Pulm, P., Titschack, J. and Troccoli, L. and Senatskommission für Ozeanographie der Deutschen Forschungsgemeinschaft, MARUM – Zentrum für Marine Umweltwissenschaften der Universität Bremen, Leitstelle Deutsche Forschungsschiffe (2012) Surface and Intermediate Water hydrography, planktonic and benthic biota in the Caribbean Sea – Climate, Bio and Geosphere linkages (OPOKA) : [Meteor] Cruise No. 78, Leg 1 February 22 – March 28, 2009, Colón (Panama) – Port of Spain (Trinidad and Tobago) Meteor-Berichte, 11-6 . Leitstelle Meteor, Institut für Meereskunde der Universität Hamburg, Hamburg, Germany, 40 pp. DOI 10.3289/cr_m78_1.

Sheinbaum, J., Candela, J., Badan, A., Ochoa, J. (2002) Flow structure and transport in the Yucatan Channel. Geophys. Res. Lett. 29(3), 1040, doi:10.1029/2001GL013990.

Steph, S., Tiedemann, R., Prange, Groeneveld, J. Nürnberg, D., Reuning, L., Schulz, M., Haug, G. H. (2006) Changes in Caribbean surface hydrography during the Pliocene shoaling of the Central American Seaway. Paleoceanography 21, PA4221, doi:10.1029/2004PA001092.

Sturges, W., Evans, J.C., Welsh, S., Holland, W. (1993) Separation of Warm-Core Rings in the Gulf of Mexico. J. Phys. Oceangr. 23 (2), 250–268.

Zavala-Hidalgo, J., Morey, S. L., O'Brien, J., Zamudio, L. (2006) On the Loop Current eddy shedding variability. Atmòsfera 19, 41-48.

11 Appendix
11.1 Lithology Logs

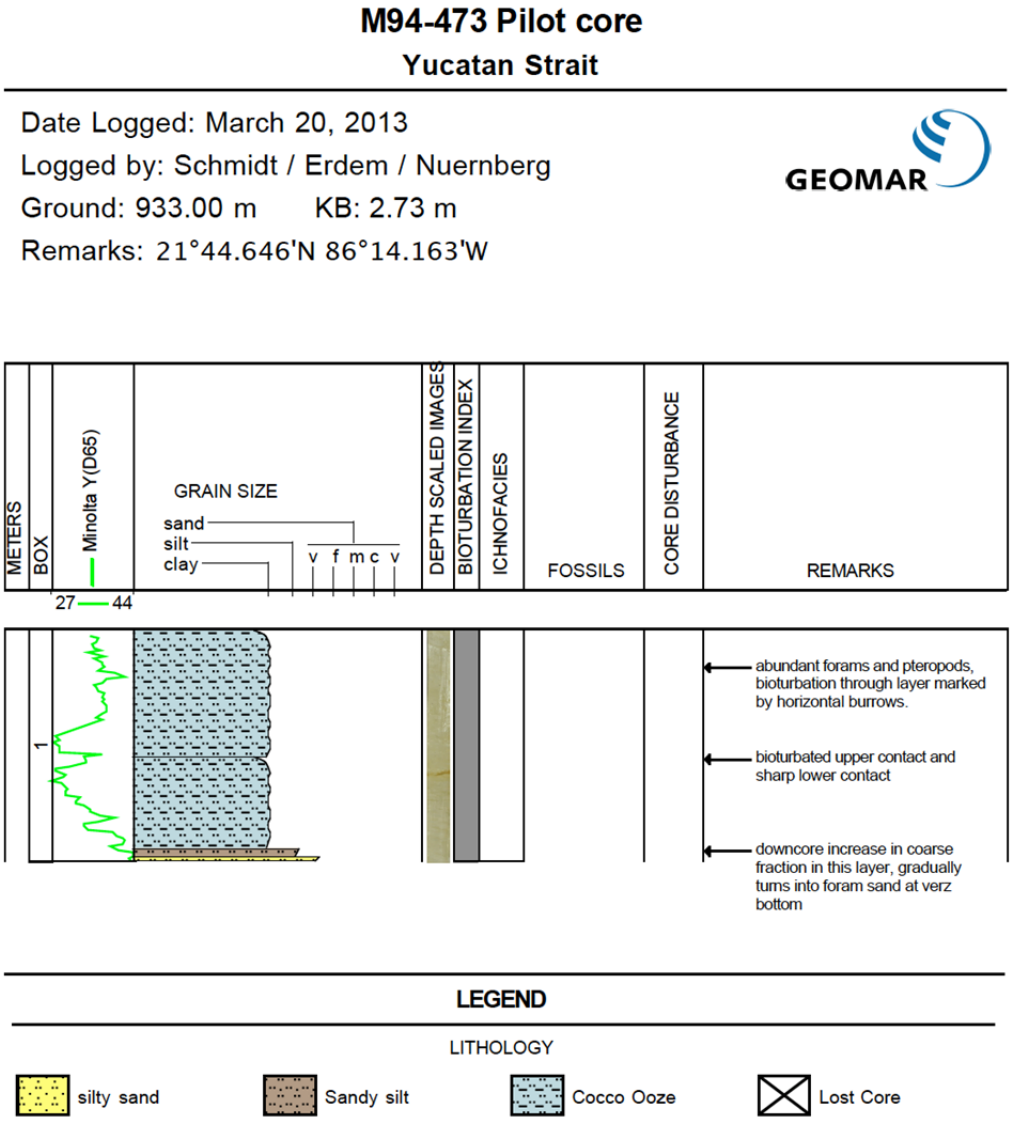

Fig. A11.1.1 Lithology log of core M94-473 Pilot Core (by AppleCORE v10.2a).

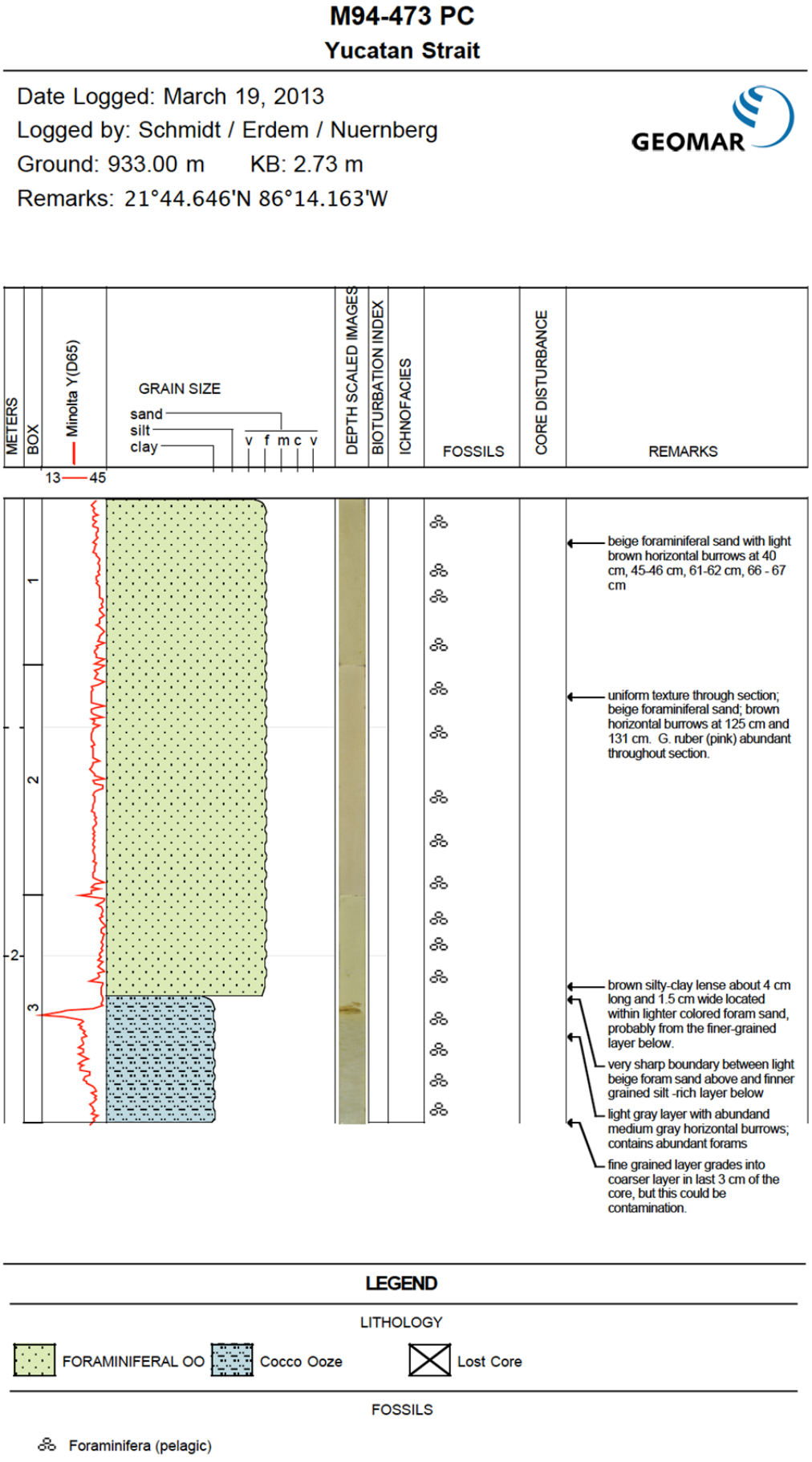

Fig. A11.1.2 Lithology log of core M94-473 Piston Core (by AppleCORE v10.2a).

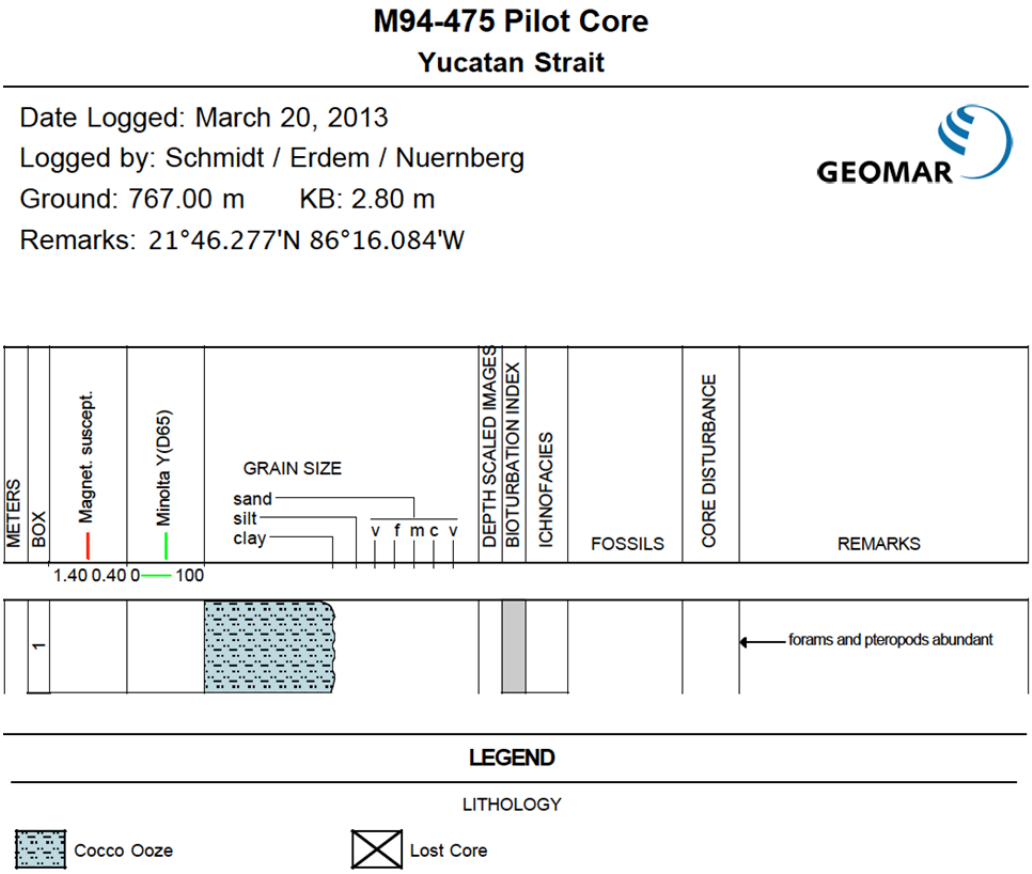

Fig. A11.1.3 Lithology log of core M94-475 Pilot Core (by AppleCORE v10.2a).

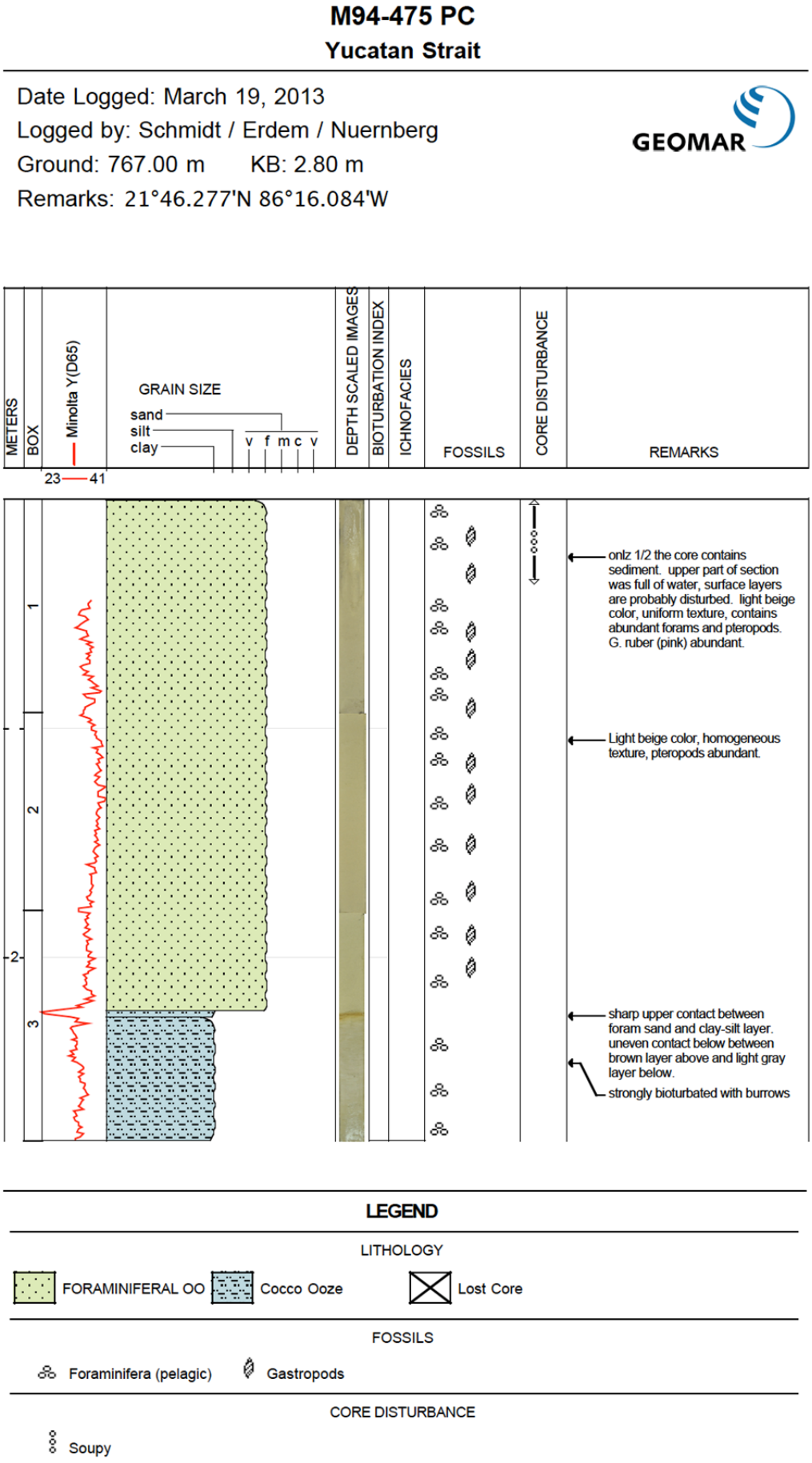

Fig. A11.1.4 Lithology log of core M94-475 Piston Core (by AppleCORE v10.2a).

M94-478 PC

southern Campeche Bank

Date Logged: March 20, 2013
Logged by: Schmidt / Erdem / Nuernberg
Ground: 749.00 m KB: 6.31 m
Remarks: 22°43.059'N 86°26.544'W

GEOMAR

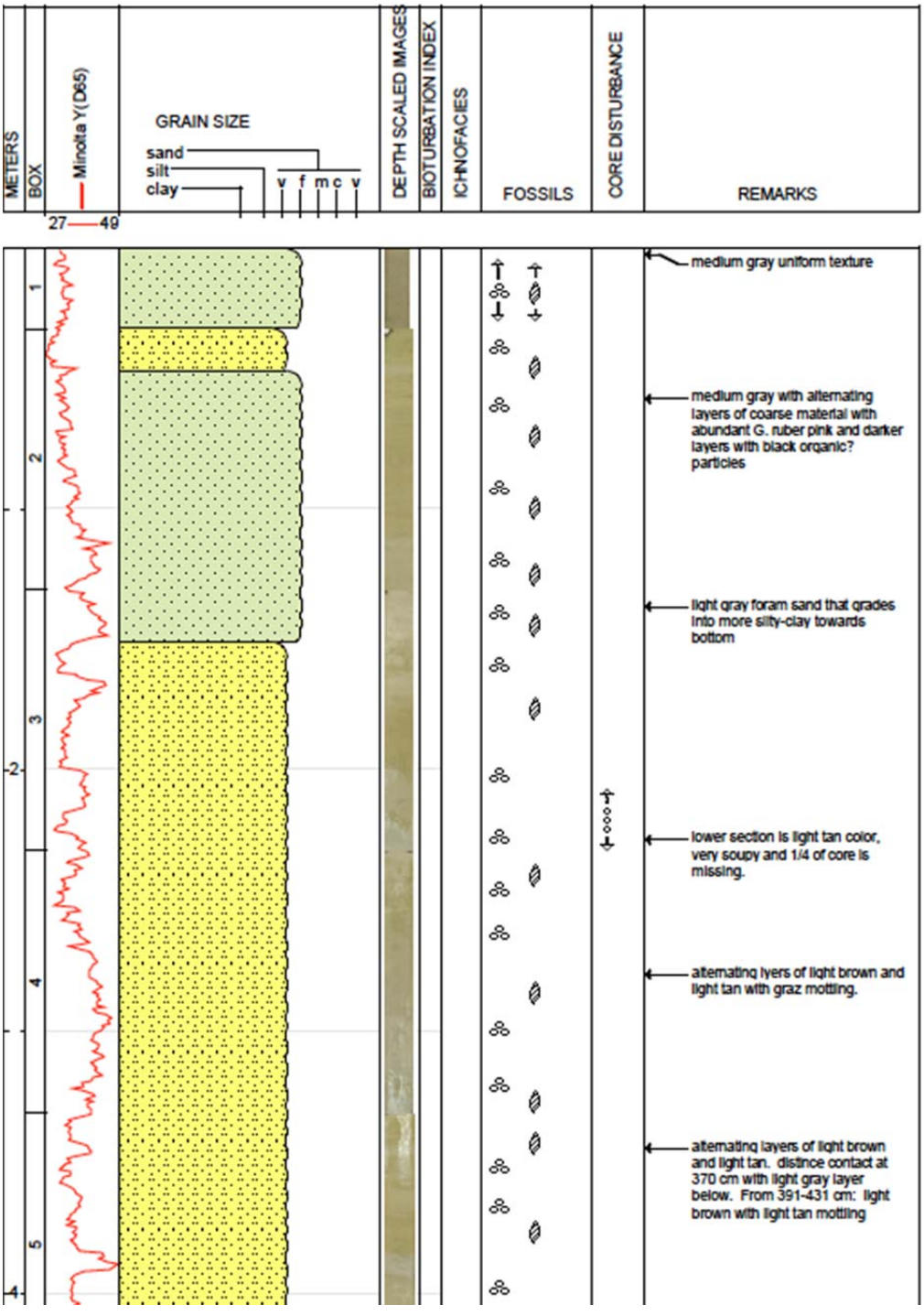

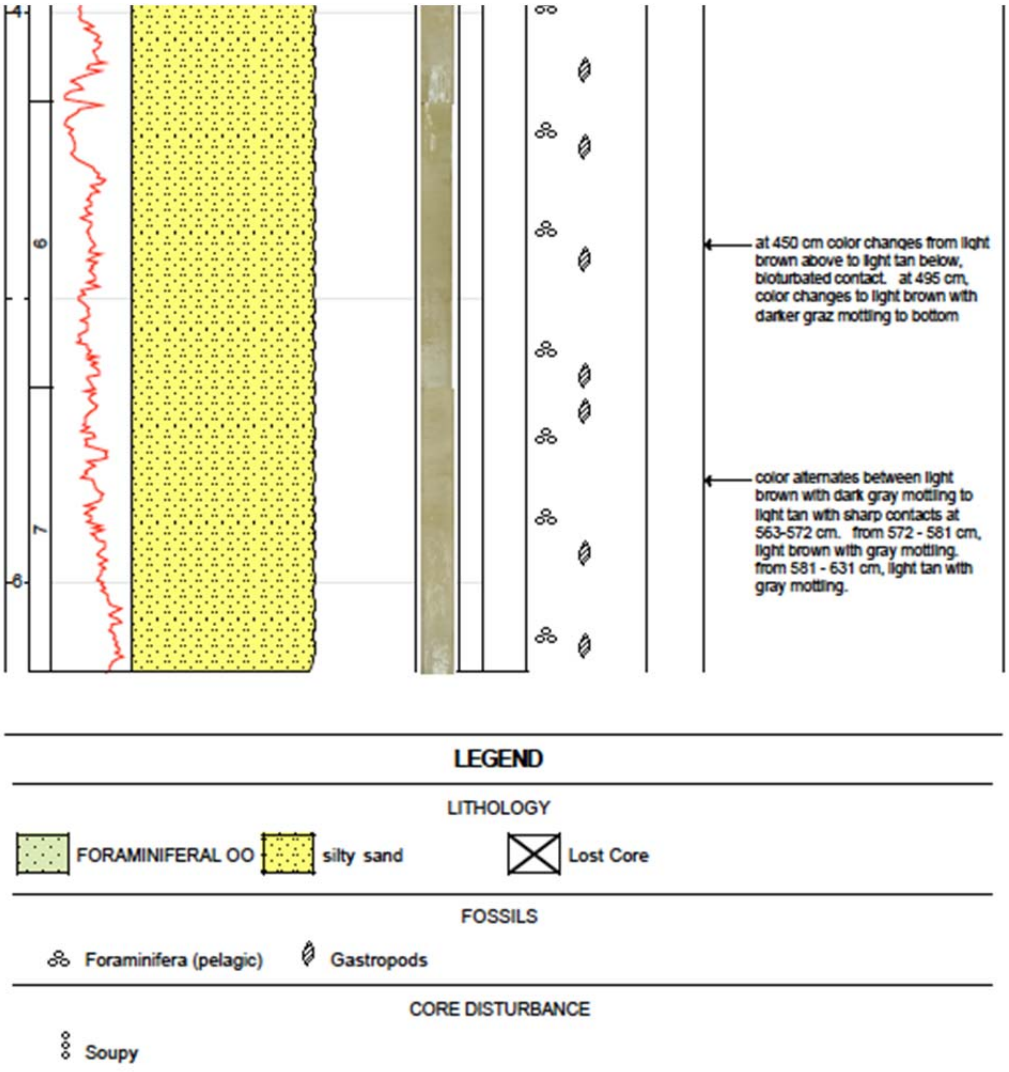

Fig. A11.1.5 Lithology log of core M94-478 Piston Core (by AppleCORE v10.2a).

M94-480 PC

deep northern Campeche Bank

Date Logged: March 23, 2013
Logged by: Schmidt / Erdem / Nuernberg
Ground: 730.00 m KB: 12.17 m
Remarks: 23°48.141'N 87°0.868'W

GEOMAR

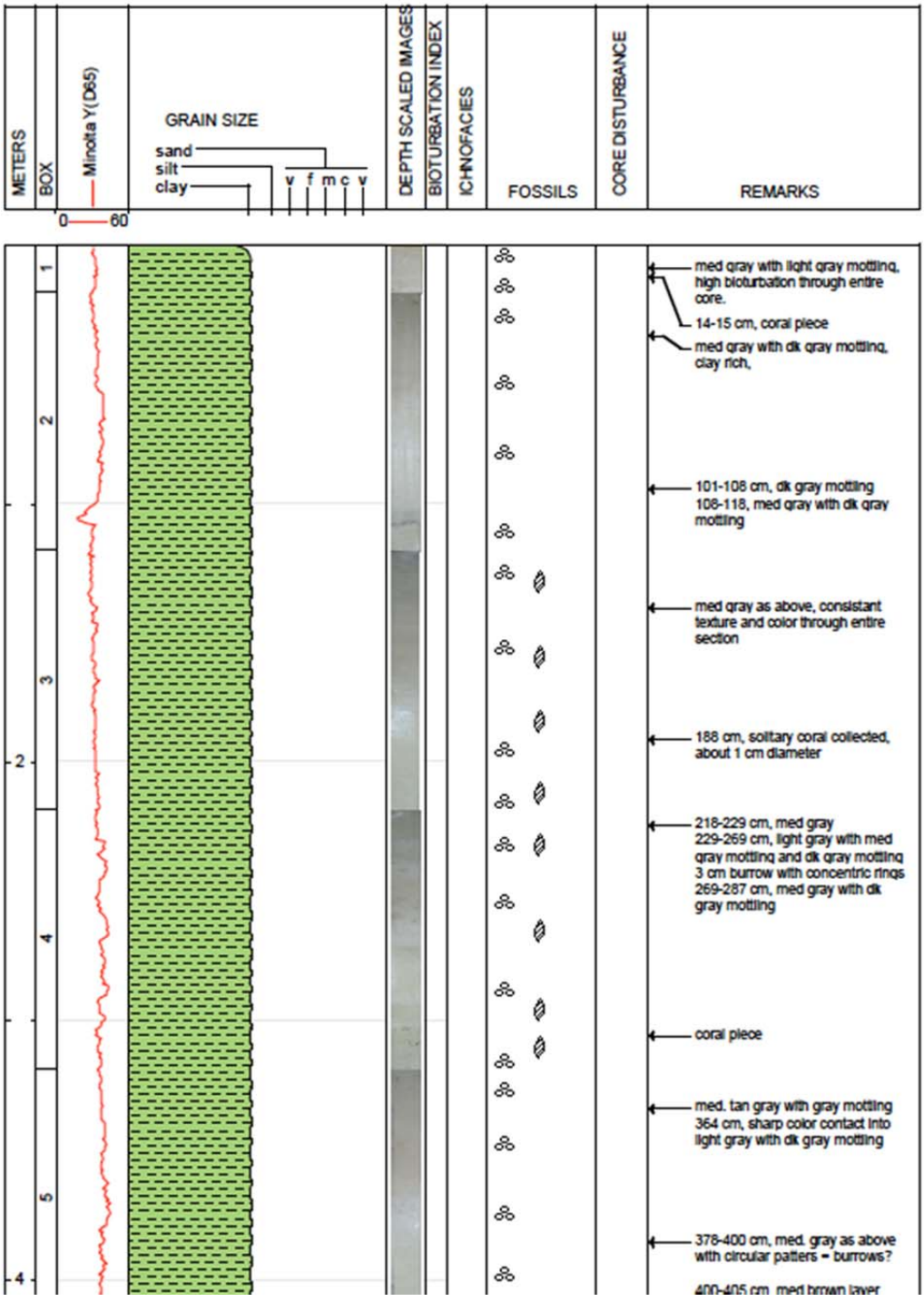

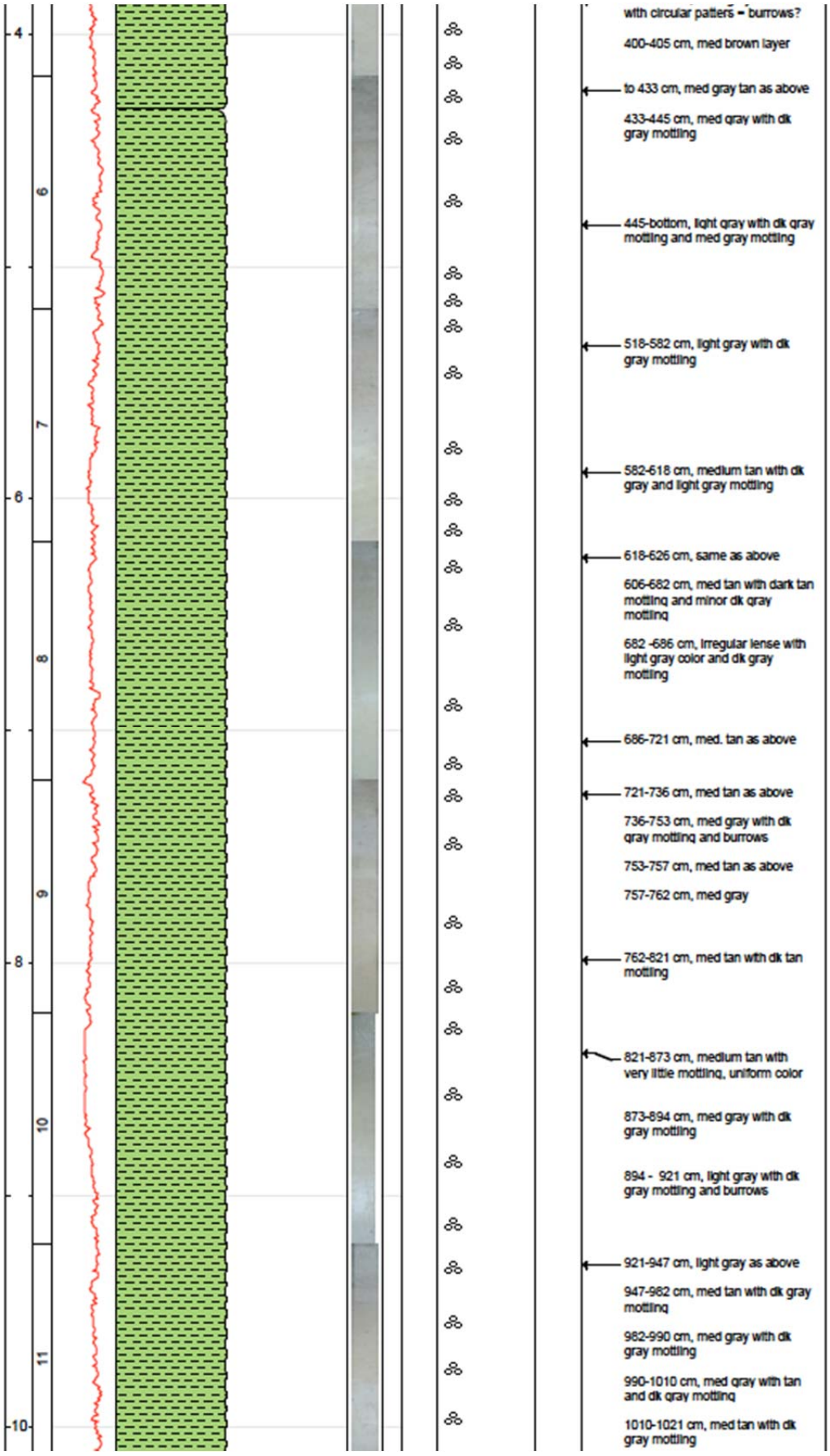
with circular patters - burrows?
400-405 cm, med brown layer
to 433 cm, med gray tan as above
433-445 cm, med qray with dk gray mottling
445-bottom, light qray with dk qray mottling and med gray mottling
518-582 cm, light gray with dk gray mottling
582-618 cm, medium tan with dk gray and light gray mottling
618-626 cm, same as above
606-682 cm, med tan with dark tan mottling and minor dk qray mottling
682 -686 cm, irregular lense with light gray color and dk gray mottling
686-721 cm, med. tan as above
721-736 cm, med tan as above
736-753 cm, med gray with dk qray mottling and burrows
753-757 cm, med tan as above
757-762 cm, med gray
762-821 cm, med tan with dk tan mottling
821-873 cm, medium tan with very little mottling, uniform color
873-894 cm, med gray with dk gray mottling
894 - 921 cm, light gray with dk gray mottling and burrows
921-947 cm, light gray as above
947-982 cm, med tan with dk gray mottling
982-990 cm, med gray with dk gray mottling
990-1010 cm, med qray with tan and dk qray mottling
1010-1021 cm, med tan with dk gray mottling

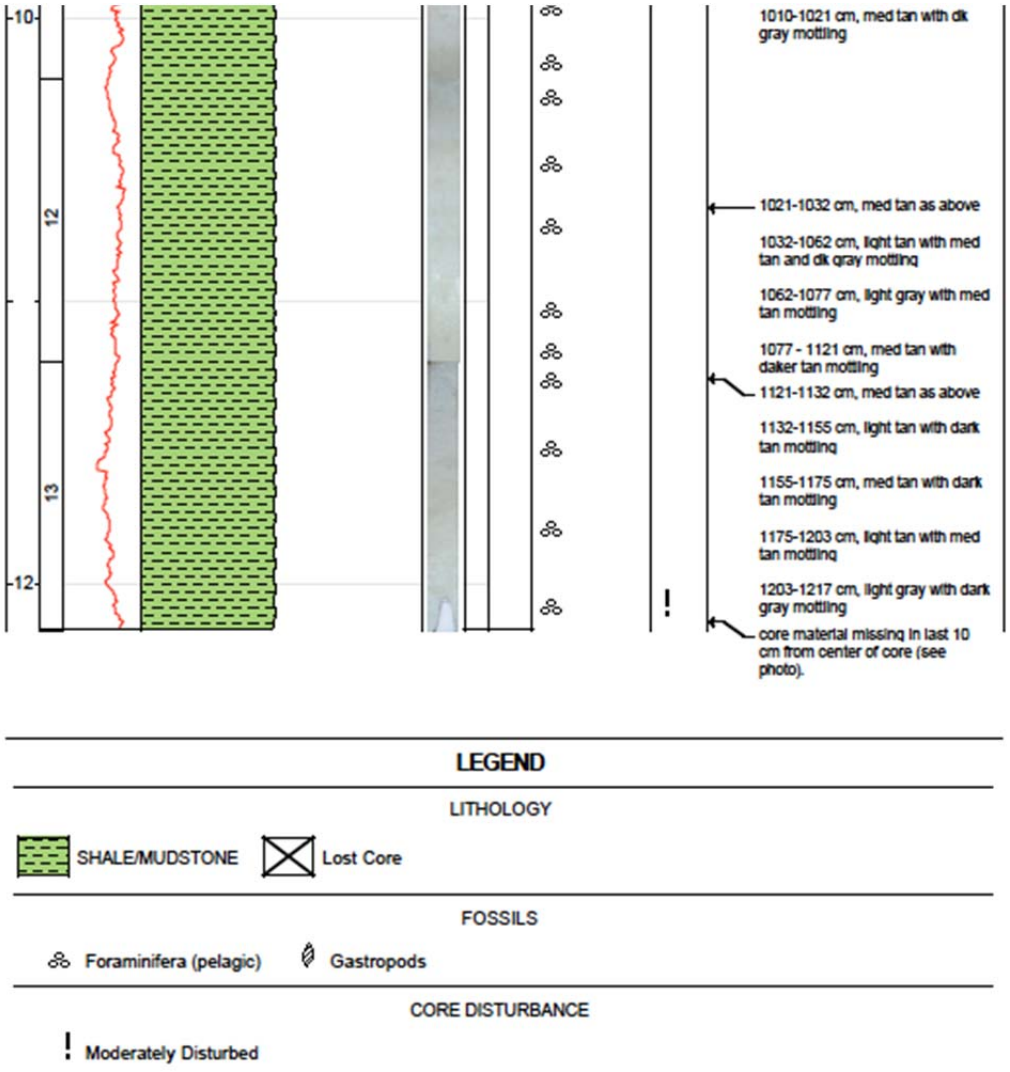

Fig. A11.1.6 Lithology log of core M94-480 Piston Core (by AppleCORE v10.2a).

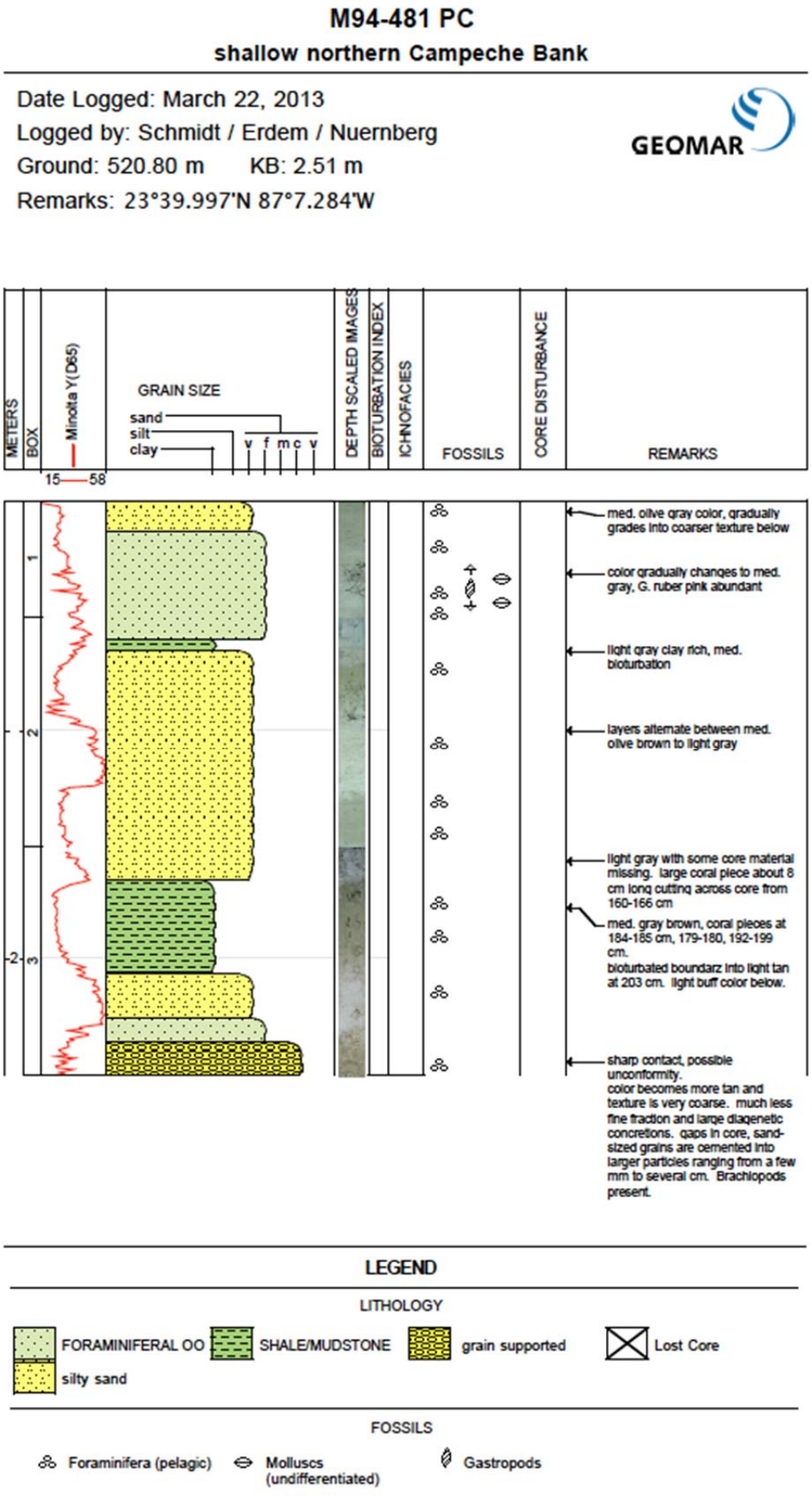

Fig. A11.1.7 Lithology log of core M94-481 Piston Core (by AppleCORE v10.2a).

M94-482 PC

mid-depth northern Campeche Bank

Date Logged: March 23, 2013
Logged by: Schmidt / Erdem / Nuernberg
Ground: 629.80 m KB: 8.81 m
Remarks: 23°49.155N 87°7.752W

GEOMAR

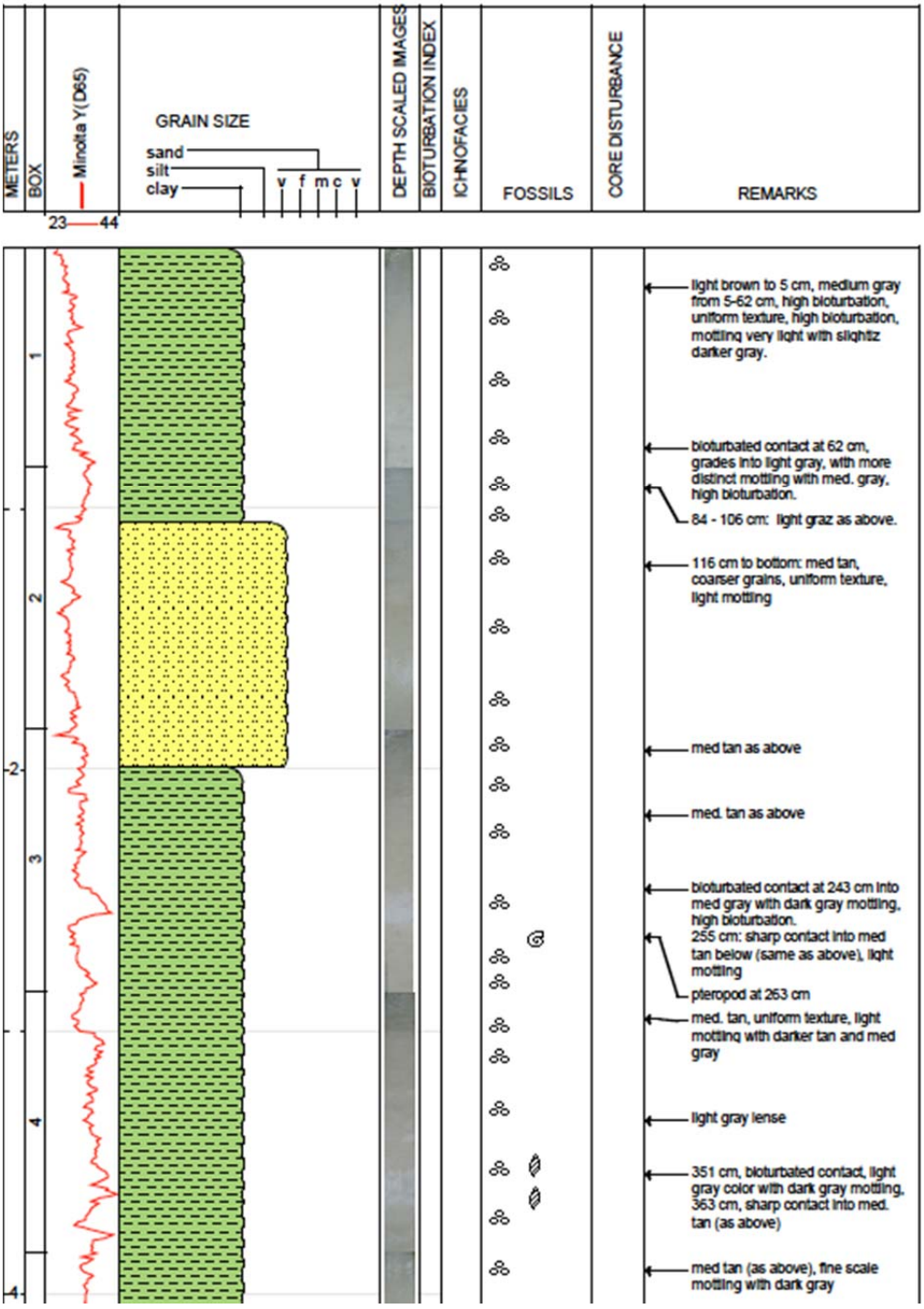

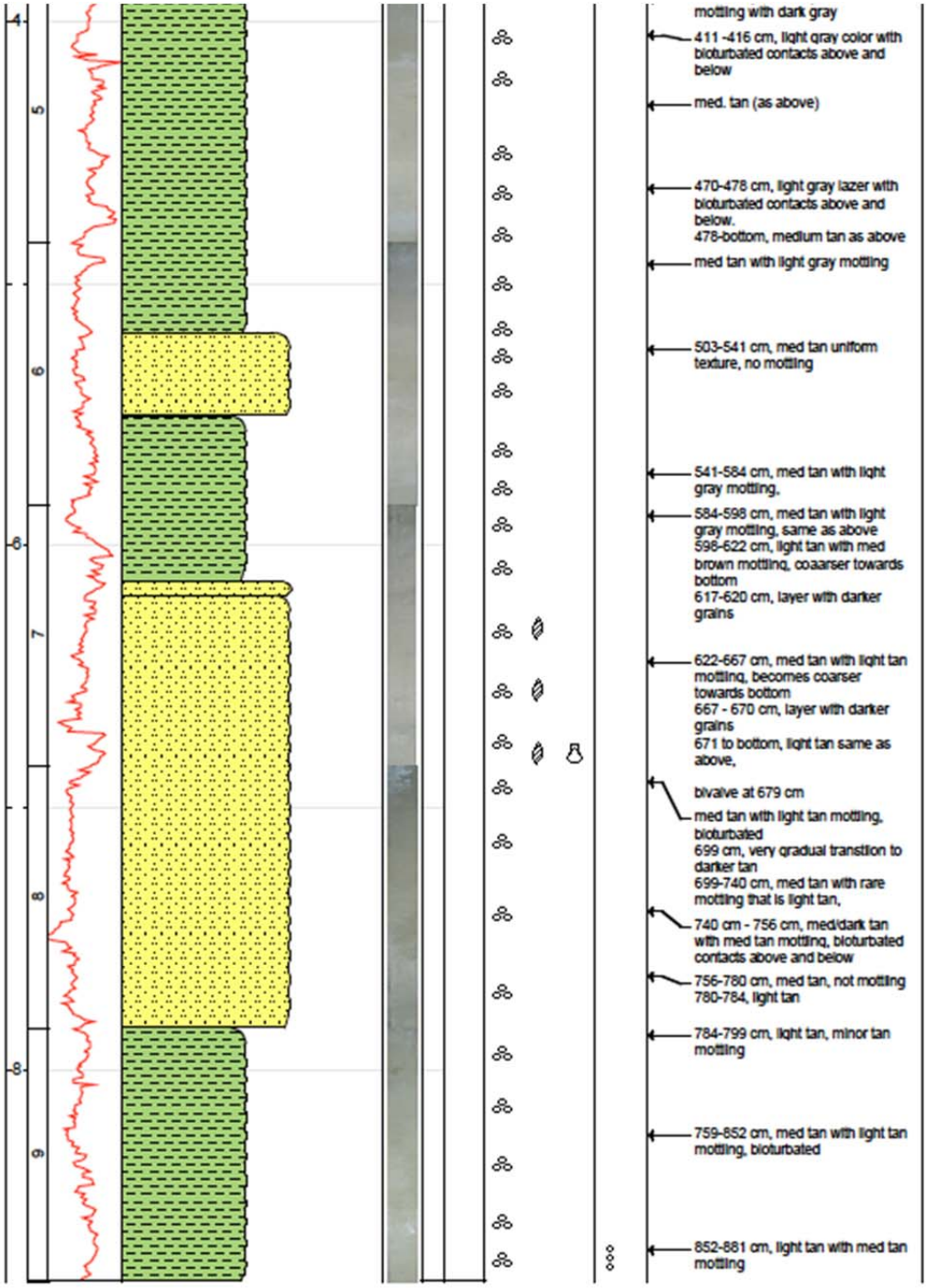

Fig. A11.1.8 Lithology log of core M94-482 Piston Core (by AppleCORE v10.2a).

11.2 Sediment Core Photography

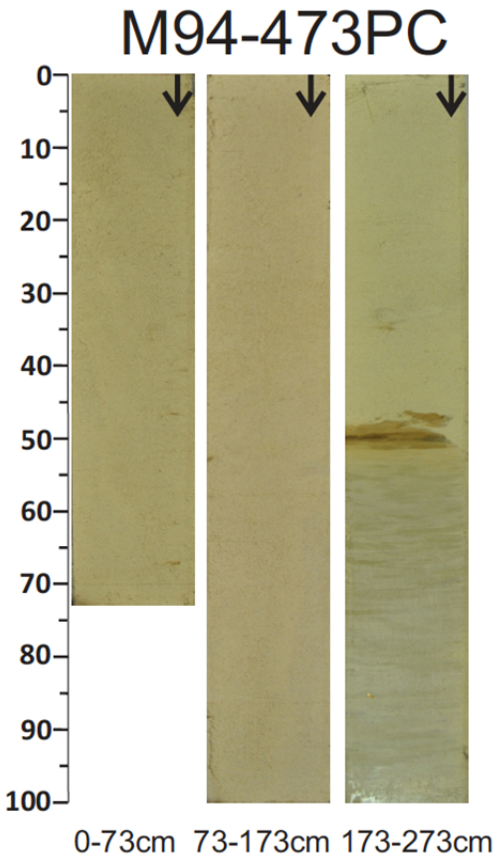

Fig. A11.2.1. Core photography of core M94-473 PC from Yucatan Strait (21°44.646 N 86°14.183 W, 933 m water depth).

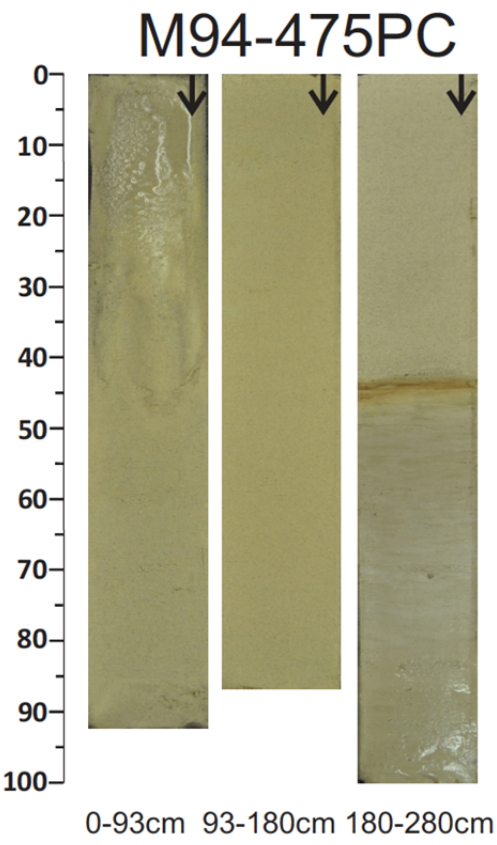

Fig. A11.2.2. Core photography of core M94-47 PC from Yucatan Strait (21°46.277 N 86°16.08 ~767 m water depth).

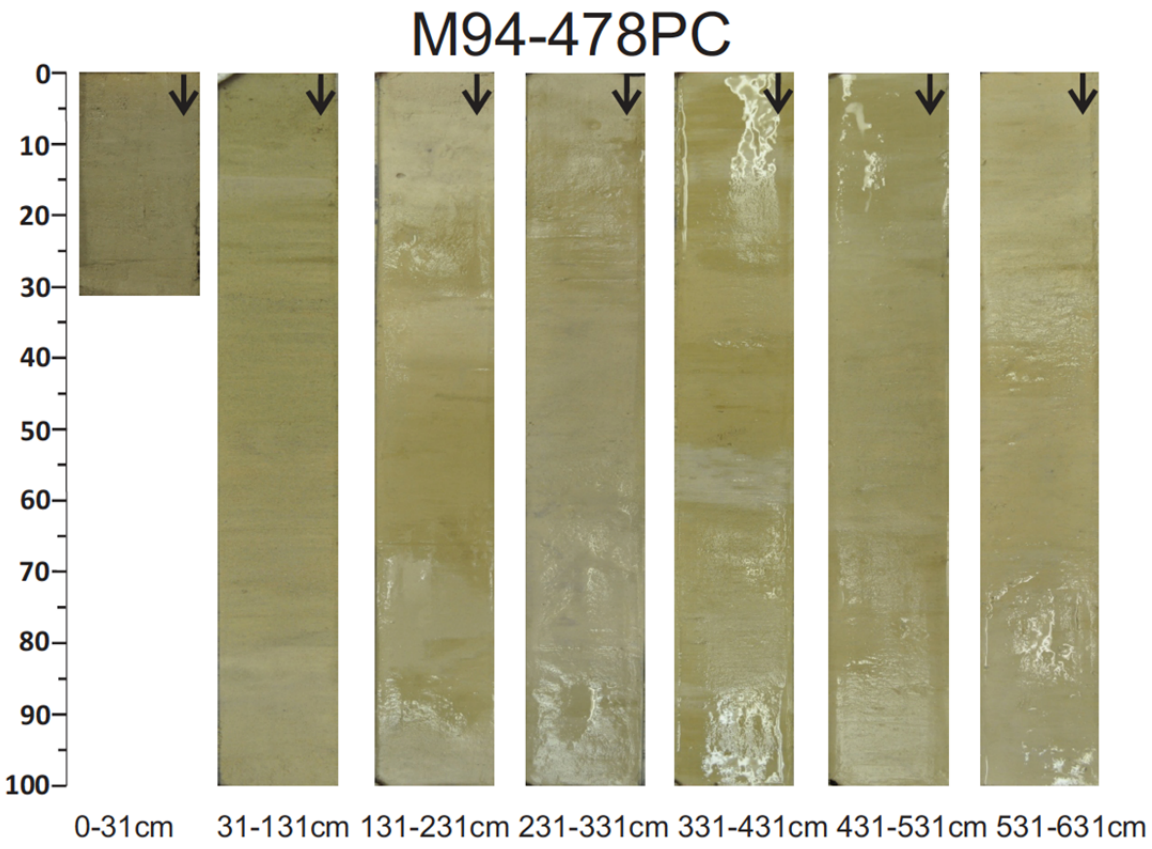

Fig. A11.2.3. Core photography of core M94-478 PC from the southern Campeche Bank (22°43.059 N 86°26.544 W, ~749 m water depth).

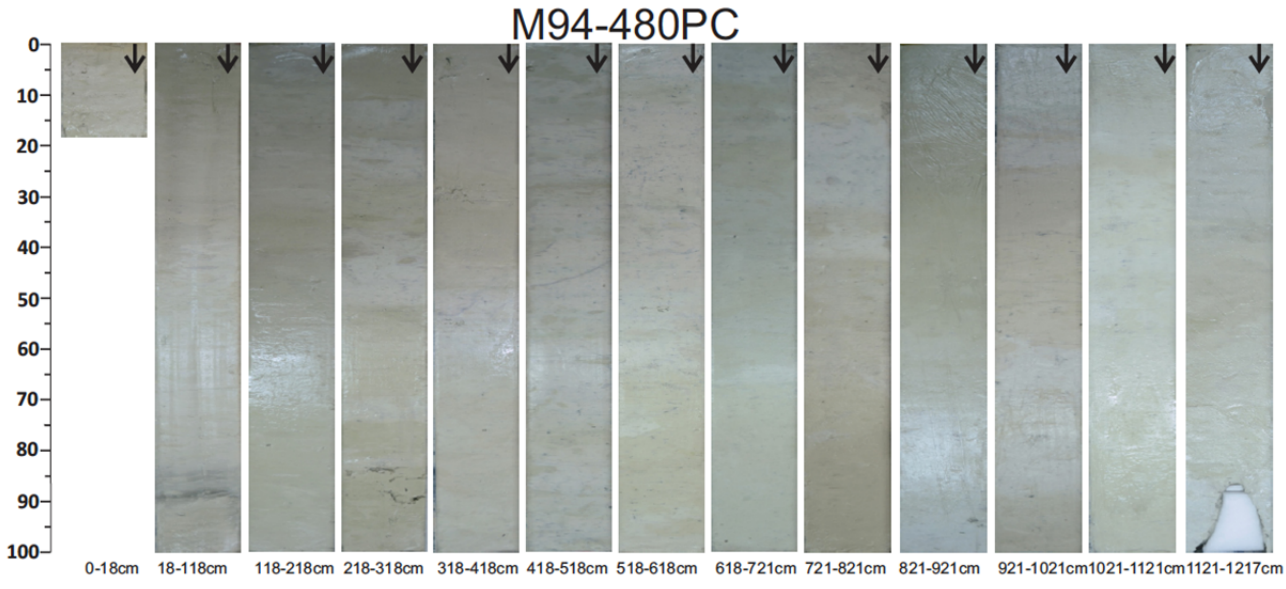

Fig. A11.2.4. Core photography of core M94-480 PC from the deep northern Campeche Bank (23°48.141 N 87°0.868 W, ~730 m water depth).

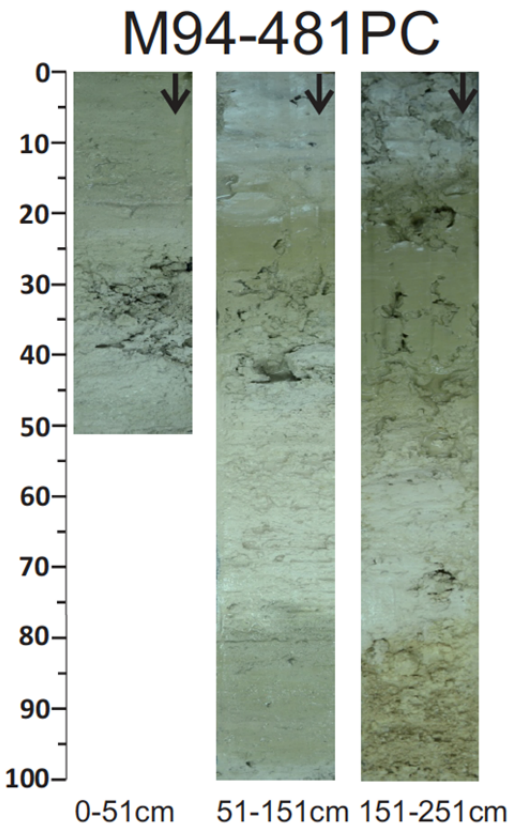

Fig. A11.2.5. Core photography of core M94-481 PC from the shallow northern Campeche Bank (23°39.997 N 87°7.284 W, ~521 m water depth).

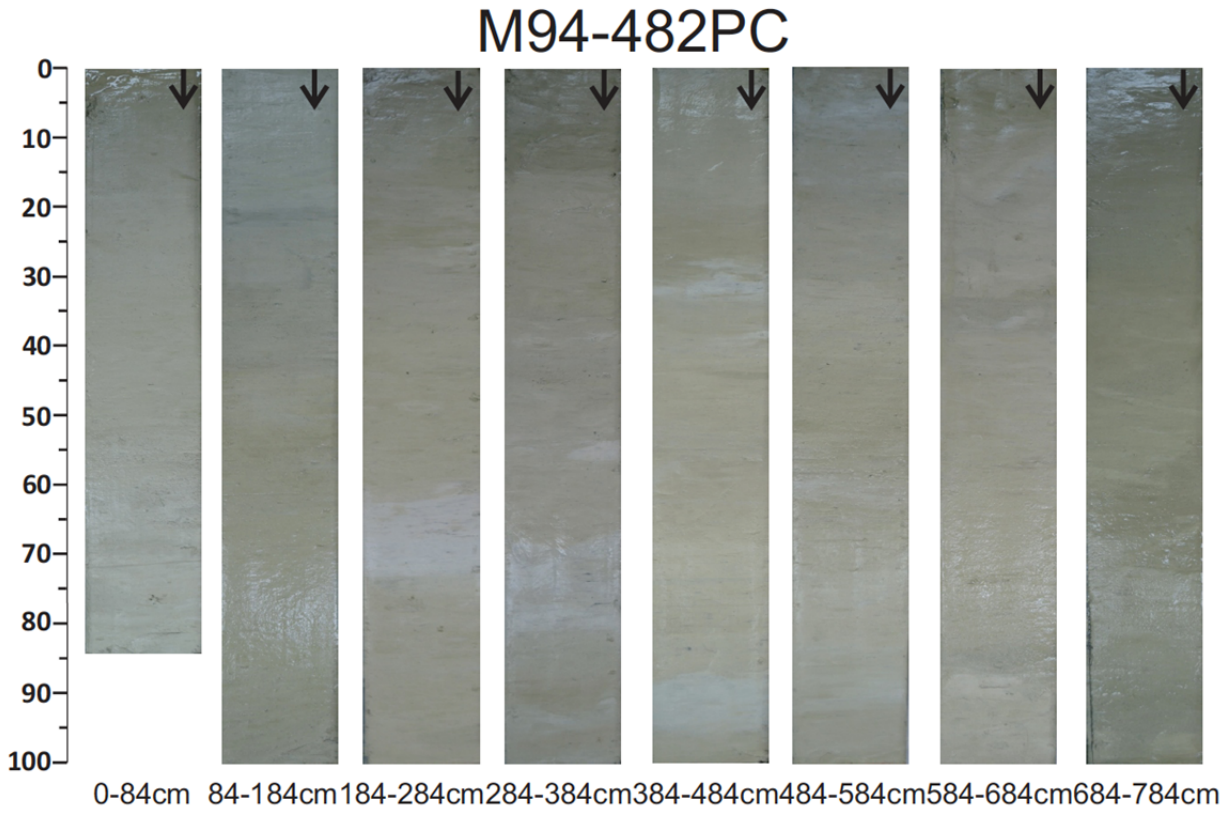

Figure A11.2.6. Core photography of core M94-482 PC from the mid-depth northern Campeche Bank (23°49.155 N 87°7.752 W, ~630 m water depth).

11.3 Sediment Color Scanning

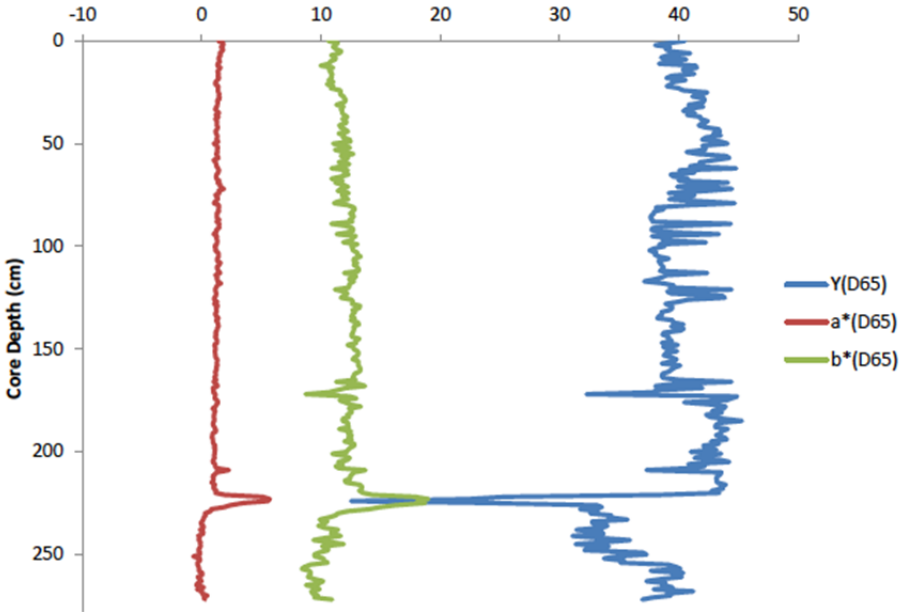

Fig. A11.3.1. Minolta color scanner data of core M94-473 PC from Yucatan Strait (21°44.646 N 86°14.163 W, 933 m water depth): Y (D65), a* and b* CIELAB color coordinates. The Y-values represent the lightness on a linear scale. The a*-values indicate the relationship between green and magenta and the b*-value reflects blue/yellow colors.

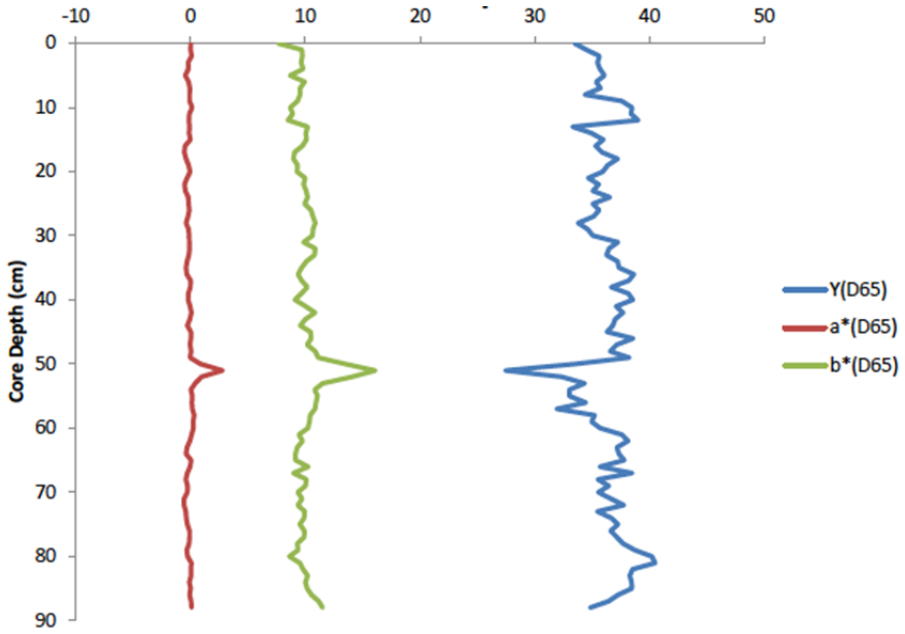

Fig. A11.3.2. Minolta color scanner data of pilot core M94-473 PC from Yucatan Strait (21°44.646 N 86°14.163 W, 933 m water depth): Y (D65), a* and b* CIELAB color coordinates. The Y-values represent the lightness on a linear scale. The a*-values indicate the relationship between green and magenta and the b*-value reflects blue/yellow colors.

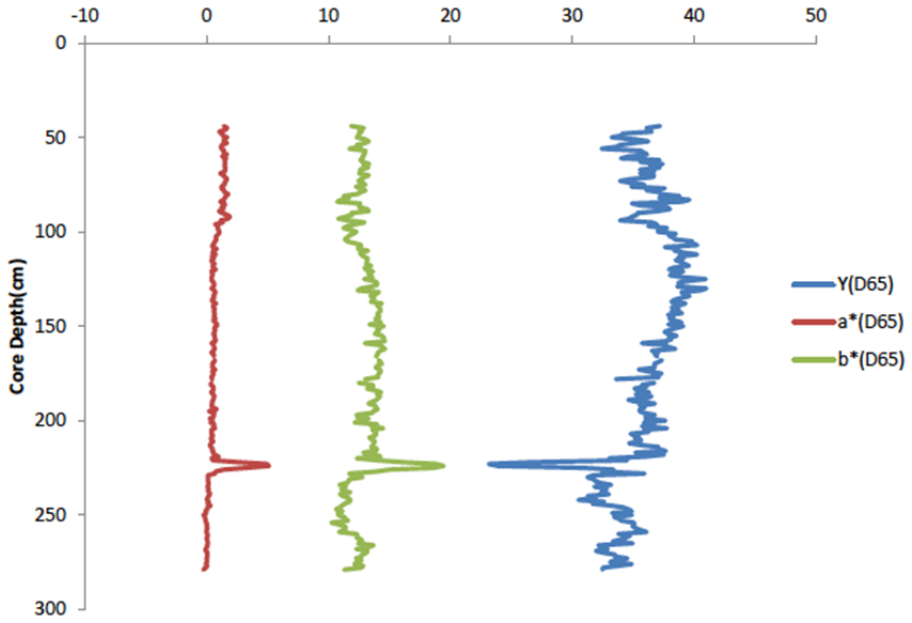

Fig. A11.3.3. Minolta color scanner data of core M94-475 PC from Yucatan Strait (21°46.277 N 86°16.084 W, 767 m water depth): Y (D65), a* and b* CIELAB color coordinates. The Y-values represent the lightness on a linear scale. The a*-values indicate the relationship between green and magenta and the b*-value reflects blue/yellow colors.

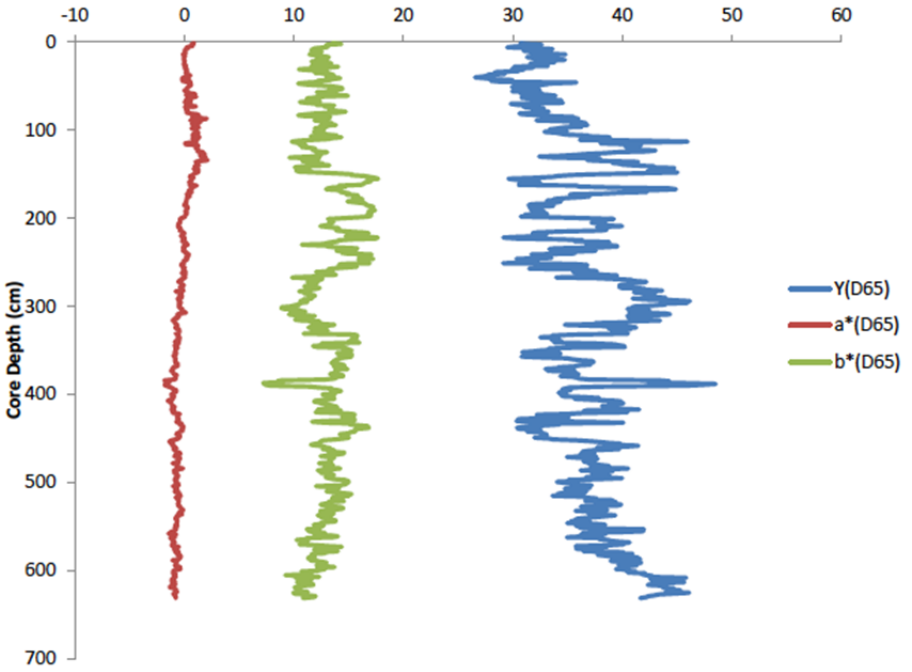

Fig. A11.3.4. Minolta color scanner data of core M94-478 PC from Yucatan Strait (22°43.059 N 86°26.544 W, 749 m water depth): Y (D65), a* and b* CIELAB color coordinates. The Y-values represent the lightness on a linear scale. The a*-values indicate the relationship between green and magenta and the b*-value reflects blue/yellow colors.

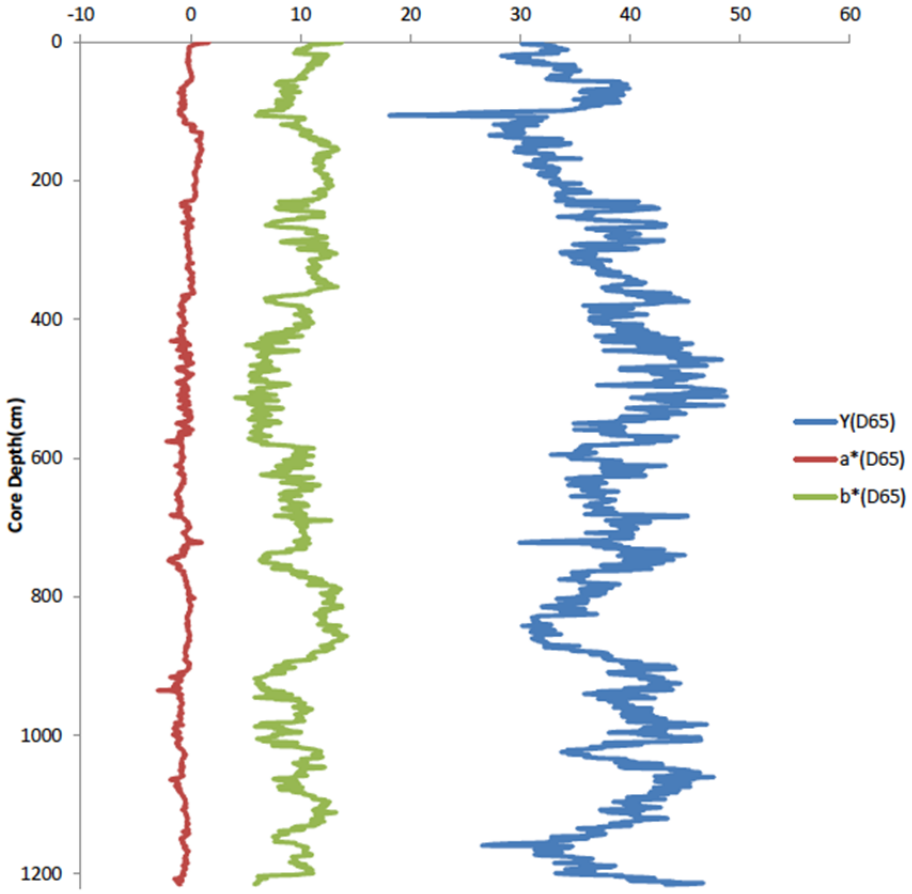

Fig. A11.3.5. Minolta color scanner data of core M94-480 PC from the northern Campeche Bank (23°48.141 N 87°0.868 W, 730 m water depth): Y (D65), a* and b* CIELAB color coordinates. The Y-values represent the lightness on a linear scale. The a*-values indicate the relationship between green and magenta and the b*-value reflects blue/yellow colors.

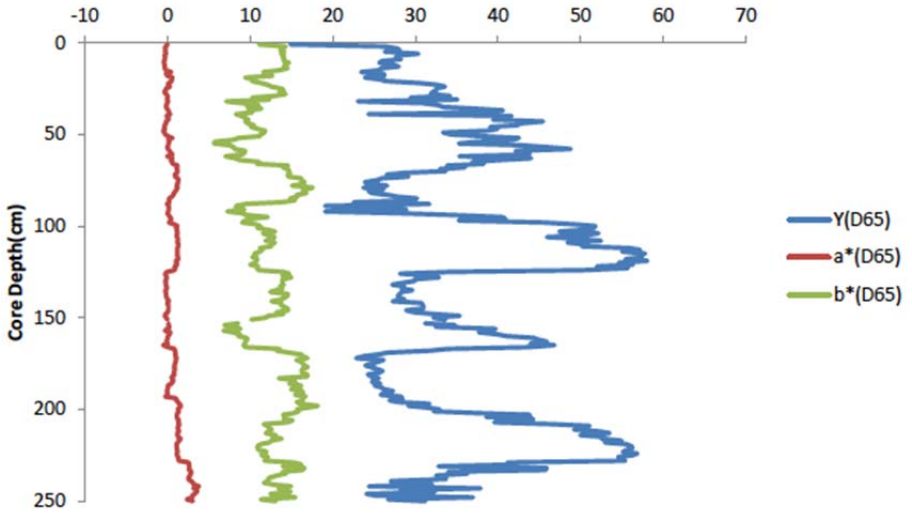

Fig. A11.3.6. Minolta color scanner data of core M94-481 PC from the northern Campeche Bank (23°39.997 N 87°7.284 W, 520 m water depth): Y (D65), a* and b* CIELAB color coordinates. The Y-values represent the lightness on a linear scale. The a*-values indicate the relationship between green and magenta and the b*-value reflects blue/yellow colors.

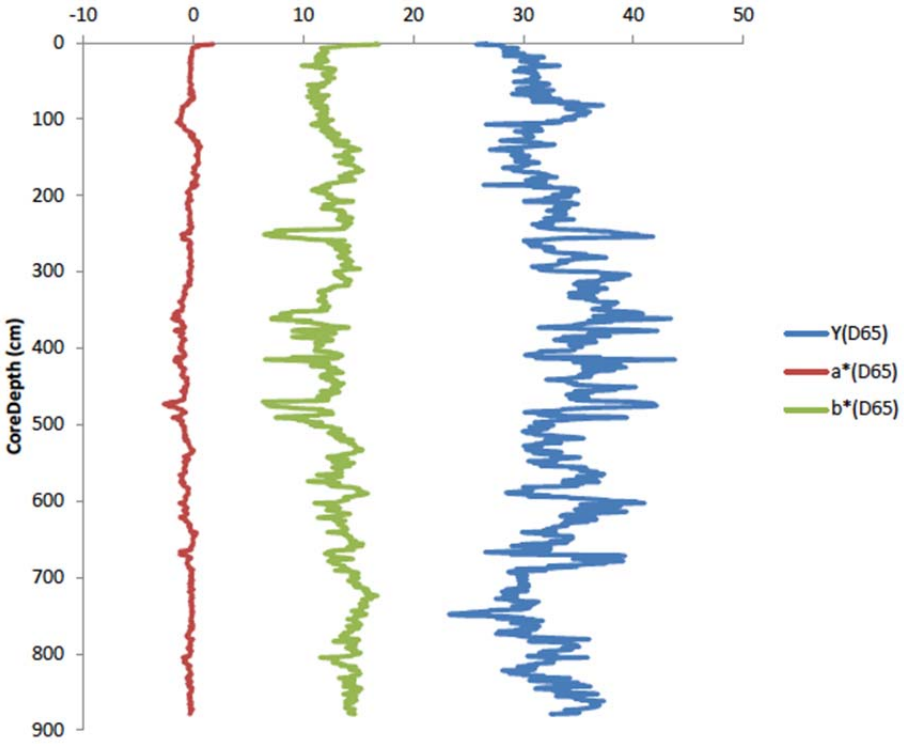

Fig. A11.3.7. Minolta color scanner data of core M94-482 PC from the northern Campeche Bank (23°49.155 N 87°7.752 W, 629 m water depth): Y (D65), a* and b* CIELAB color coordinates. The Y-values represent the lightness on a linear scale. The a*-values indicate the relationship between green and magenta and the b*-value reflects blue/yellow colors.